

Benchmarking Physics-Informed Time-Series Models for Operational Global Station Weather Forecasting

Tao Han^{1,2} Zhibin Wen³ Zhenghao Chen⁴ Dazhao Du¹ Song Guo¹ Lei Bai²

Abstract

The development of Time-Series Forecasting (TSF) models is often constrained by the lack of comprehensive datasets, especially in Global Station Weather Forecasting (GSWF), where existing datasets are small, temporally short, and spatially sparse. To address this, we introduce WEATHER-5K, a large-scale observational weather dataset that better reflects real-world conditions, supporting improved model training and evaluation. While recent TSF methods perform well on benchmarks, they lag behind operational Numerical Weather Prediction systems in capturing complex weather dynamics and extreme events. We propose PhysicsFormer, a physics-informed forecasting model combining a dynamic core with a Transformer residual to predict future weather states. Physical consistency is enforced via pressure–wind alignment and energy-aware smoothness losses, ensuring plausible dynamics while capturing complex temporal patterns. We benchmark PhysicsFormer and other TSF models against operational systems across several weather variables, extreme event prediction, and model complexity, providing a comprehensive assessment of the gap between academic TSF models and operational forecasting. The dataset and benchmark implementation are available at: <https://github.com/taohan10200/WEATHER-5K>.

1. Introduction

Global Station Weather Forecasting (GSWF) is essential for providing precise and timely weather information, with significant implications across various sectors.

¹Hong Kong University of Science and Technology, Hong Kong
²Shanghai AI Laboratory, China ³Southern University of Science and Technology, China ⁴The University of Newcastle, Australia
 . Correspondence to: Song Guo <songguo@ust.hk>, Lei Bai <bailei@pjlab.org.cn>.

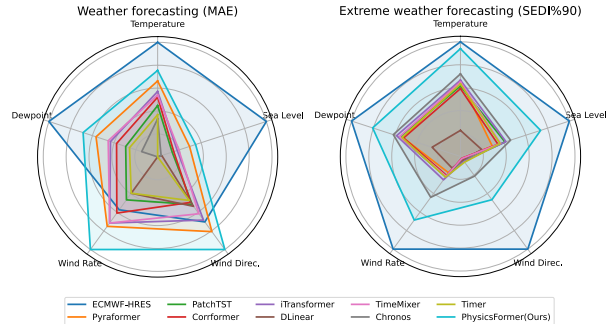


Figure 1. Comparison of the operational NWP model and various TSF models across five weather variables. On the left-hand side, the prediction comparison is based on the MAE metric, and on the right-hand side, it focuses on predictions under extreme weather conditions. In both cases, we take the reciprocal so that a larger area indicates better performance.

The mainstream approach for precise station-based weather forecasting is Numerical Weather Prediction (NWP), which can be categorized into physically-based (Phillips, 1956; Lynch, 2008) and data-driven models (Lam et al., 2023; Bi et al., 2023; Chen et al., 2023; Han et al., 2024a). Physically-based NWPs solve partial differential equations describing atmospheric dynamics, while data-driven NWPs leverage historical weather data with advanced machine learning to improve accuracy. Despite their reliability, NWP models are computationally intensive, requiring substantial resources for data assimilation, medium-range forecasting, and interpolation to produce station-specific predictions.

Time-Series Forecasting (TSF) methods provide a lightweight alternative by directly learning from historical station observations, enabling end-to-end predictions without complex interpolation. TSF approaches have recently shown strong performance on small-scale station datasets; for example, (Zhou et al., 2022; Zeng et al., 2023; Liu et al., 2024b; Wang et al., 2024; Murad et al., 2024) achieve high accuracy in temperature forecasting on the Weather dataset¹. These results highlight the potential of TSF as a computationally efficient and scalable alternative to NWP for station-level forecasting. In this work, we systematically evaluate this potential through a comprehensive benchmark.

¹<https://www.bgc-jena.mpg.de/wetter>

In addition, to combine the efficiency of TSF with physical consistency, physics-informed methods (Sel et al., 2023; Nagda et al., 2025; Nasiri et al., 2026) have been explored. Building on this, we propose PhysicsFormer, which integrates dynamic core into a Transformer backbone and enforces physics constraints via the loss function, aiming to capture complex dynamics and extreme events while remaining computationally efficient.

1.1. Knowledge Gap and Motivations

We first identify four major limitations (L1–L4) as follows:

L1: Inadequate Data Scale and Diversity for Global Generalization. Current TSF methods for GSWF are limited by small, homogeneous datasets. Many datasets focus on a single station (Wu et al., 2021), a localized region (Godahewa et al., 2021), or short timeframes (Wu et al., 2023), which restricts models’ ability to generalize. As a result, these models typically excel only in short-term forecasts, such as one-day predictions. Even though recent work has introduced end-to-end GSWF models (Wu et al., 2023), the lack of comprehensive datasets remains a major bottleneck.

L2: Disconnect Between Academic TSF Models and Real-world Forecasting. Though state-of-the-art TSF methods excel under ideal conditions (e.g., short lead times) on academic benchmarks, their real-world deployment remains limited. This gap highlights the need for an enhanced benchmark that aligns with operational challenges, captures the complexities of real-world weather systems (Wu et al., 2021; Zhou et al., 2021), and bridges the divide between academic research and practical application.

L3: Insufficiently Operational Evaluation Metrics. The evaluation of TSF methods for GSWF often relies on limited metrics such as Mean Squared Error (MSE) (Wu et al., 2021; Nie et al., 2023; Liu et al., 2021), which focus solely on overall accuracy. This overlooks key aspects of weather forecasting, such as the prediction of extreme events such as heatwaves, storms, or strong winds, that are vital for real-world applications. Moreover, factors like model complexity are usually not considered, resulting in an incomplete assessment of real-world forecasting performance.

L4: Ignoring Physical Dynamics in Current TSF Methods. Existing TSF methods (Wang et al., 2024; Murad et al., 2024) often ignore physical dynamics, such as pressure–wind relationships and energy conservation. This limits forecasting accuracy and extreme event prediction.

1.2. Contribution and Innovation

Motivated by these limitations, we introduce WEATHER-5K, a new benchmark enabling operational TSF models, along with an enhanced evaluation framework using operational metrics for fair assessment. We further propose

PhysicsFormer, a physics-informed TSF model. Our key contributions (C1–C4) are summarized below:

C1: A Comprehensive Global Dataset, WEATHER-5K. WEATHER-5K addresses L1 by providing extensive training data from 5,672 weather stations worldwide, spanning 10 years of hourly observations. Its broad coverage and diverse conditions allow TSF methods to generalize across regions and time scales.

C2: Enhanced Operational Benchmarking with NWP Comparisons. To address L2, our benchmark evaluates a wide range of TSF models, including Transformer-, MLP-, GNN-based methods, and LTMs, against operational NWP models over longer lead times and diverse real-world scenarios, extending beyond prior work (Wu et al., 2023).

C3: Operational Evaluation Metrics. To address L3, we introduce the *Symmetric Extremal Dependence Index (SEDI)* for extreme event prediction and incorporate a complexity metric to assess efficiency and operational feasibility, providing a comprehensive operational evaluation.

C4: Physics-Informed Forecasting. To address L4, we propose PhysicsFormer, a physics-informed Transformer that integrates dynamic core and enforces physics constraints via the loss function, improving real-world applicability, and forecast accuracy.

2. Taxonomy of TSF Methods

This study categorizes the recent TSF models into four types: We classify TSF models into four types: (a) MLP-based models (b) Transformer-based models (c) GNN-based models and (d) large time-series models (LTMs) capable for evaluating capable of zero-shot prediction.

MLP-based models. Many MLP-based forecasting models have been proposed due to their architectural simplicity (Oreshkin et al., 2019; Challu et al., 2023). STID (Shao et al., 2022) shows that a simple MLP can outperform sophisticated GNN models in spatio-temporal forecasting, while DLinear (Zeng et al., 2023) demonstrates that linear projections may surpass Transformer-based models. SparseTSF (Lin et al., 2024) exploits Cross-Period Sparse Forecasting to improve efficiency, while TimeMixer (Wang et al., 2024) and WPMixer (Murad et al., 2024) capture multi-resolution temporal information. Due to their high computational efficiency, these MLP-based models are particularly suitable for edge-side deployment.

Transformer-based models. The Transformer architecture (Vaswani et al., 2017) has become a prevalent backbone for TSF, giving rise to numerous variants. Informer (Zhou et al., 2021), Autoformer (Wu et al., 2021), Pyraformer (Liu et al., 2021), and FEDformer (Zhou et al., 2022) aim to improve efficiency for long-sequence modeling through sparse

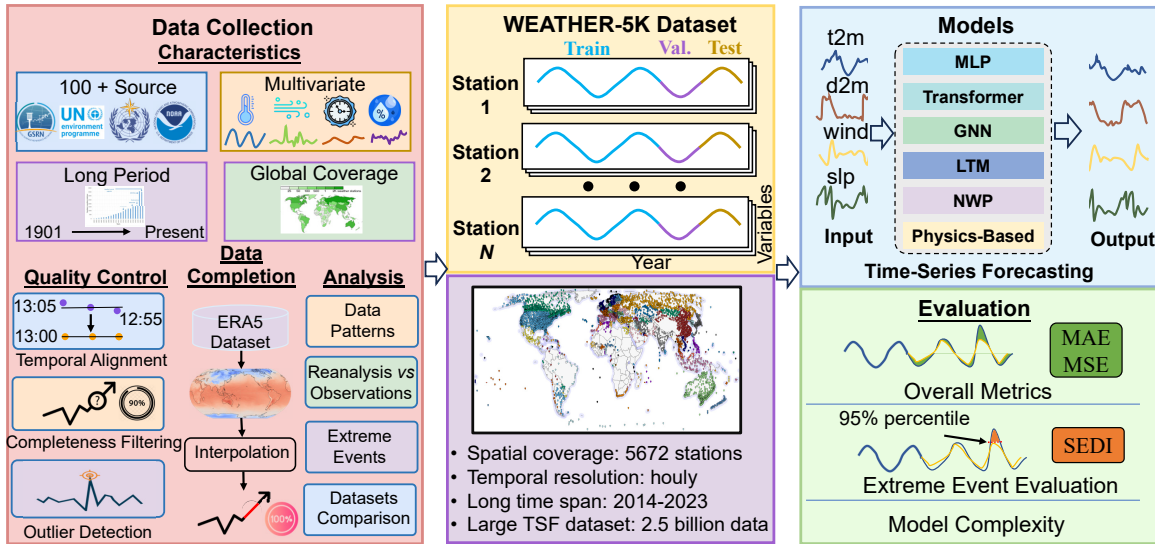


Figure 2. The flow diagram of the WEATHER-5K dataset and the benchmark.

attention designs. PatchTST (Nie et al., 2023) enhances efficiency and performance by embedding time series as patches within a standard Transformer. iTransformer (Liu et al., 2024b) models inter-variable dependencies by treating each variable as a token. Corrformer (Wu et al., 2023) is tailored for worldwide weather station forecasting, explicitly capturing spatial and temporal correlations.

GNN-based models. Graph Neural Networks (GNNs) are effective for modeling interactions in multivariate time series by representing variables as nodes and relationships as edges. In spatio-temporal forecasting, GNNs are often combined with RNNs or TCNs, as exemplified by DCRNN (Li et al., 2018), AGCRN (Bai et al., 2020), and STGCN (Han et al., 2020). To reduce reliance on predefined graph structures, MTGNN (Wu et al., 2020) and DGCRN (Li et al., 2023) learn adjacency matrices adaptively. Despite their strong performance in domains such as traffic forecasting, GNN-based models face scalability and computational challenges when applied to large-scale graphs.

Large time series models (LTMs). Motivated by the success of large language models (LLMs) in NLP (Raffel et al., 2020; Achiam et al., 2023), recent work explores their application to time-series forecasting or develops specialized large time series models (Liang et al., 2024). Some approaches directly adapt pre-trained LLMs for time series (Zhou et al., 2023; Jin et al., 2023; Xue & Salim, 2023; Liu et al., 2024c), but their zero-shot performance is often limited and typically requires task-specific fine-tuning. To address this, recent studies pre-train large time series models from scratch on large-scale time series datasets (Liu et al., 2024d; Goswami et al., 2024; Ansari et al., 2024). Representative examples include Chronos (Ansari et al., 2024), which adopts a T5-based (Raffel et al., 2020) lan-

guage model architecture for tokenized time series, and Timer (Liu et al., 2024d), which trains an autoregressive Transformer on large-scale forecasting data. These models exhibit improved zero-shot forecasting performance.

3. WEATHER-5K Dataset

3.1. Collection and Pre-processing

Data source. WEATHER-5K is derived from global near-surface in-situ observations, which is achieved in the publicly available Integrated Surface Database (ISD), leveraging data from high-quality observation networks. ISD is a global repository of hourly and synoptic surface observations, which encompasses a wide range of meteorological parameters, such as the wind speed and direction, temperature, dew point, and sea level pressure.

Station selection. ISD contains records from over 20,000 stations spanning 1901-present. though certain stations are no longer operational, many do not report data on an hourly basis, and numerous stations have missing values for critical weather elements. To enhance data quality, a meticulous selection process was conducted to include only long-term, hourly reporting stations currently operational and provide essential observations. As a result, 10,701 stations continuously operate from 2014 to 2024.

3.2. Quality Control

A high-quality dataset is crucial for TSF. As shown in Figure 2, WEATHER-5K has been subjected to rigorous post-processing and quality control to ensure data reliability.

Data interpretation. In ISD, meteorological variables are

Table 1. Statistics of different time-series datasets. ‘N/A’ means the dataset is not publicly available.

Dataset	Domain	Frequency	Lengths	Stations	Variables	Year	Volume
Exchange (Lai et al., 2018)	Exchange	1 day	7,588	1	8	1990-2010	623KB
Electricity (Trindade, 2015)	Electricity	1 hour	26,304	321	1	2016-2019	92MB
ETm2 (Zhou et al., 2021)	Electricity	15 mins	57,600	1	7	2016-2018	9.3MB
Traffic (Wu et al., 2021)	Traffic	1 hour	17,544	862	1	2016-2018	131MB
LargeST-CA (Liu et al., 2024a)	Traffic	5 mins	525,888	8600	1	2017-2021	36.8GB
Solar (Lai et al., 2018)	Weather	10 mins	52,560	137	1	2006	8.3MB
Wind (Li et al., 2022)	Weather	15 mins	48,673	1	7	2020-2021	2.7MB
Weather (Wu et al., 2021)	Weather	10 mins	52,696	1	21	2020	7.0MB
Weather-Australia (Godahewa et al., 2021)	Weather	1 day	1,332~65,981	3,010	4	unknown	202MB
GlobalTempWind (Wu et al., 2023)	Weather	1 hour	17,544	3,850	2	2019-2020	1034MB
CMA.Wind (Wu et al., 2023)	Weather	1 hour	17,520	34,040	1	2018-2019	N/A
WEATHER-5K (Ours)	Weather	1 hour	87,648	5672	5	2014-2023	40.0GB

encoded as strings rather than floating-point values, with each string containing the numerical measurement along with metadata such as quality flags and reporting types. For example, a temperature entry $\langle +0130, 1 \rangle$ denotes a temperature of 13.0 C° at the first quality level. Following the official ISD guidelines, all variables are systematically parsed into standardized numerical formats suitable for analysis and storage.

Temporal alignment. Although selected stations nominally report hourly data, timestamps may deviate slightly from exact hours (e.g., 12:55 or 13:05 instead of 13:00). To address this issue, we estimate missing hourly values using the nearest observations within a 30-minute window, substantially improving hourly coverage. For the small fraction of hours still missing due to the absence of nearby observations, linear interpolation is applied using data from the surrounding 12 consecutive hours to maintain temporal consistency.

Completeness filtering. From the 10,701 candidate stations, we retain only those with more than 90% valid hourly records. This filtering yields 5,672 stations worldwide, covering the period from 2014 to 2023, and balances long-term operation, hourly data availability, and coverage of diverse meteorological variables.

Outlier detection. Outliers are identified through an examination of temporal dynamics, targeting observations that fall far outside plausible ranges or exhibit anomalous behavior relative to the majority of records. We employ a combination of statistical methods and machine learning algorithms to distinguish genuine extremes from noise or data errors.

3.3. Data Completion and Statistics

After quality control, only a small fraction of data points remain missing, primarily due to long-term gaps at certain stations (e.g., exceeding one day). Since complete station records are required for spatial modeling in TSF, we fill remaining gaps using the ERA5 reanalysis dataset (Hers-

bach et al., 2018) at station locations. Given that ERA5 is a widely used high-quality global reanalysis product, this interpolation introduces minor errors, with the largest impact expected for high-frequency variables such as wind speed.

To support model training on WEATHER-5K, we compute the decadal mean and variance of each variable for input standardization (see Appendix Table 6). In addition, motivated by the limited evaluation of extremes in existing TSF benchmarks, we calculate station-wise percentiles at 90%, 95%, 98%, and 99.5% for each variable, enabling the assessment of extreme-value forecasting performance.

3.4. Analysis

We provide a detailed analysis of WEATHER-5K, including station density, different data patterns, comparisons with ERA5, and extreme events such as heatwaves, in Appendix D. Briefly, the WEATHER-5K dataset exhibits notable regional disparities in station coverage, heterogeneous temporal patterns across variables, and a more accurate representation of real-world weather conditions compared to reanalysis data ERA5. In particular, it better captures extreme events, including heatwaves, which ERA5 tends to underestimate. In addition, Table 1 compares WEATHER-5K with widely used TSF datasets and highlights key limitations of existing benchmarks. (1) *Small scale and outdated.* Mainstream TSF datasets (Lai et al., 2018; Trindade, 2015; Wu et al., 2021) remain limited in scale and temporal coverage. For example, commonly used electricity consumption and exchange-rate datasets are sparse or outdated, constraining the practical applicability of forecasting models. (2) *Lagging behind other fields.* Compared to domains such as vision and language, where large-scale datasets (e.g., Common Crawl and LAION-5B (Schuhmann et al., 2022)) have driven substantial scientific and economic progress, the TSF community has been slow to adopt large-scale data. Until recently, only one large-scale time-series dataset, LargeST (Liu et al., 2024a), has been introduced.

Benchmarking Physics-Informed Time-Series Models for Operational Global Station Weather Forecasting

Table 2. Benchmarks on our WEATHER-5K. The results are based on 4 different prediction lengths: 24, 72, 120, and 168, and the input length is 48. For each method, we report the average results across all prediction lengths and the full results can be found in the Appendix Table 8 and Table 9. ECMWF-HRES is the physical-based NWP model, representing the most accurate weather forecasting model. Underline is the second-best performance.

Type	Method	Temperature		Dewpoint		Wind Rate		Sea Level Pressure	
		MAE	MSE	MAE	MSE	MAE	MSE	MAE	MSE
NWP (Operational)	ECMWF-HRES	1.94	8.56	2.06	9.96	1.56	5.00	1.29	5.17
Transformer-based	Informer (2021 AAAI)	2.75	15.20	2.87	17.98	1.52	4.88	4.17	40.63
	Autoformer (2021 NIPS)	2.82	16.44	2.98	18.41	1.55	5.20	4.17	41.46
	Pyraformer (2022 ICLR)	2.49	13.49	2.68	15.82	<u>1.51</u>	<u>4.87</u>	3.72	34.32
	FEDformer (2022 ICML)	2.85	16.84	2.98	19.07	1.57	5.20	4.03	37.82
	PatchTST (2023 ICLR)	2.84	17.18	3.07	20.47	1.59	5.35	4.27	44.40
	Corrformer (2023 NMI)	2.72	15.17	2.95	18.22	1.55	5.00	4.22	43.43
	iTransformer (2024 ICLR)	2.64	15.24	2.87	18.34	1.52	4.96	4.11	42.12
MLP-based	STID (2022 CIKM)	4.71	41.40	4.22	35.06	1.69	6.29	5.77	64.64
	DLinear (2023 AAAI)	3.57	23.71	3.49	23.38	1.61	5.32	4.60	46.28
	SparseTSF (2024 ICML)	3.24	20.53	3.15	21.43	1.66	5.80	4.98	54.70
	TimeMixer (2024 ICLR)	2.69	15.38	2.84	17.82	1.52	4.99	4.06	39.69
	WPMixer (2025 AAAI)	2.79	16.50	2.94	18.85	1.56	5.20	4.20	41.43
GNN-based	MTGNN (2020 KDD)	10.33	171.74	9.54	149.24	2.10	8.28	7.00	88.51
LTMs	Chronos (2024 TMLR)	3.03	20.76	3.28	24.57	1.72	6.64	4.62	53.58
	Timer (2024 ICML)	2.97	18.63	3.12	21.01	1.61	5.55	4.73	51.76
Physics-based	PhysicsFormer (Ours)	<u>2.34</u>	<u>11.86</u>	<u>2.51</u>	<u>14.01</u>	1.44	4.55	<u>3.53</u>	<u>32.41</u>

WEATHER-5K further addresses this gap by providing a large-scale, up-to-date observational weather dataset.

4. TSF Benchmarks on WEATHER-5K

4.1. Problem Definition

Considering N weather stations around the world and each station collects V meteorological variables, the data of all weather stations can be represented by a spatial-temporal time-series $X \in \mathbb{R}^{N \times T \times V}$ for a given look-back window of fixed length T . At timestamp t , time-series forecasting is to predict $\hat{X}_{t+1:t+\tau} = \{X_{t+1}, \dots, X_{t+\tau}\}$ based on the past T frames $X_{t-T+1:t} = \{X_{t-T+1}, \dots, X_t\}$. Here, τ is the length of the forecast horizon. Using X and \hat{X} to represent the observation data and the forecasted data, respectively, the process of GSWF can be simplified by a mapping: $\hat{X} = \mathcal{M}(X)$, where \mathcal{M} can be different kinds of time-series forecasting methods. For example, by setting $N = 1$ and ignoring the spatial information, many state-of-the-art time-series forecasting methods (Li et al., 2022; Zhou et al., 2021; Liu et al., 2021; Wu et al., 2021; Zhou et al., 2022; Gu & Dao, 2023; Wang et al., 2024; Nie et al., 2023; Liu et al., 2024b) can be explored on this task. When N is multiple scattered stations, methods (Wu et al., 2023; 2020; Shao et al., 2022) based on spatial-temporal modeling can also be applied to this task.

4.2. Baselines

We compare 16 latest baselines, covering both temporal-only and spatio-temporal TSF models, which are categorized as follows:

1) Transformer-based methods, including popular transformer-based long-term forecasting models from 2021 to 2024: Informer (2021) (Zhou et al., 2021), Autoformer (2021) (Wu et al., 2021), Pyraformer (2021) (Liu et al., 2021), FEDformer (2022) (Zhou et al., 2022), PatchTST (2023) (Nie et al., 2023), iTransformer (2024) (Liu et al., 2024b), and Corrformer (2023) (Wu et al., 2023).

2) MLP-based models: STID (2022) (Shao et al., 2022), DLinear (2023) (Zeng et al., 2023), SparseTSF (2024) (Lin et al., 2024), TimeMixer (2024) (Wang et al., 2024), and WPMixer (2025) (Murad et al., 2024).

3) GNN-based model: MTGNN (2020) (Wu et al., 2020) is included to explore graph-based weather modeling.

4) LTMs: Large time series models such as Chronos (2024) (Ansari et al., 2024) and Timer (2024) (Liu et al., 2024d) are also evaluated on WEATHER-5K.

5) Physical-based NWP: Numerical Weather Prediction model: ECMWF’s HRES (EC), a globally leading weather forecasting system, is included in WEATHER-5K for evaluation. It requires no training, Its forecast products at corresponding time steps are downloaded and interpolated to the

station locations in WEATHER-5K for assessment.

4.3. Physics-Informed Transformer

Our model, PhysicsFormer, is a hybrid framework that combines a Transformer encoder–decoder with physics-informed modeling to improve spatiotemporal weather forecasting. The model predicts future states by combining: (1) a dynamic core, which provides explicit physically-driven updates based on simplified atmospheric momentum and thermodynamic equations, and (2) a Transformer residual, which learns to correct unresolved patterns and numerical errors. Physics-informed regularization is incorporated through (i) structured input embeddings encoding geospatial and temporal information, and (ii) physics-based losses enforcing weak consistency among meteorological variables.

Global Station Spatiotemporal Encoding. Each weather station is associated with both dynamic observation data and static geographical location. We compute an embedding for global stations observation data $X_{t-T+1:t} \in \mathbb{R}^{B \times N \times T \times V}$:

$$E_{t-T+1:t} = \text{Emb}_{\text{var}}(X_{t-T+1:t}) + \text{Emb}_{\text{geo}}(\Lambda, \Phi) + \text{Emb}_{\text{time}}(\bar{T}) \in \mathbb{R}^{B \times N \times D} \quad (1)$$

where: $\text{Emb}_{\text{var}}(\cdot)$ encodes the historical sequences of V variables by flattening the temporal and variable dimensions for each station and projecting them via an MLP. $\text{Emb}_{\text{geo}}(\cdot)$ encodes the static latitude and longitude $\Lambda, \Phi \in \mathbb{R}^{B \times N}$ using Fourier features followed by an MLP. $\text{Emb}_{\text{time}}(\cdot)$ captures temporal periodicity by averaging the look-back window time markers (e.g., month, day, weekday, hour) and applying Fourier feature encodings with an MLP projection.

Spatiotemporal Interaction Modeling. Given the global station embeddings $E_{t-T+1:t}$, we apply a Transformer encoder to model interactions among global stations:

$$H_{\text{enc}} = \text{Encoder}(E_{t-T+1:t}) \in \mathbb{R}^{B \times N \times D} \quad (2)$$

Through self-attention, the encoder enables global information flow across stations, capturing global spatial interactions and large-scale atmospheric dependencies. The decoder receives the recent historical observations of length L and the encoder output to generate future predictions:

$$Z_{\text{dec}} = \text{Decoder}(E_{\text{dec}}, H_{\text{enc}}) \in \mathbb{R}^{B \times N \times D} \quad (3)$$

where E_{dec} is embedded in the same way as the encoder input.

Physics-Guided Residual Forecasting. The decoder output is mapped to a residual correction $\Delta X_{t+1:t+\tau}^{\text{res}}$ over the dynamic core forecast:

$$\Delta X_{t+1:t+\tau}^{\text{res}} = \text{Proj}(Z_{\text{dec}}) \in \mathbb{R}^{B \times N \times \tau \times V} \quad (4)$$

Here, $X_{t+1:t+\tau}^{\text{phys}}$ denotes the dynamic core output, obtained by integrating simplified atmospheric dynamics (e.g., momentum and thermodynamic equations) from the current observed state. The final forecast is then computed as:

$$\hat{X}_{t+1:t+\tau} = X_{t+1:t+\tau}^{\text{phys}} + \Delta X_{t+1:t+\tau}^{\text{res}} \quad (5)$$

This formulation ensures that the Transformer only predicts residuals, while the dynamic core enforces the main physical evolution.

Physics-Informed Training Objective. To ensure physically consistent forecasts, we augment the standard mean squared error with weak physical regularization terms.

1) Data Fidelity. We supervise predictions using the observed values at each time step:

$$\mathcal{L}_{\text{data}} = \sum_{i,t} \|\hat{X}_{i,t} - X_{i,t}\|_2^2 \quad (6)$$

2) Pressure–Wind Consistency. Atmospheric pressure drives wind motion. We enforce temporal alignment between pressure and wind variations:

$$\mathcal{L}_{\text{pw}} = \sum_{i,t} \|\Delta_t P_{i,t} - \alpha \Delta_t V_{i,t}\|_2^2 \quad (7)$$

where $P_{i,t}$ and $V_{i,t}$ denote the pressure and wind speed at station i and time t , Δ_t is the first-order temporal difference, and α is a learnable scalar.

3) Energy-Aware Smoothness. Meteorological variables evolve smoothly over time; abrupt fluctuations are penalized using a second-order difference:

$$\mathcal{L}_{\text{smooth}} = \sum_{i,t} \left(\|\Delta_t^2 T_{i,t}\|_2^2 + \|\Delta_t^2 V_{i,t}\|_2^2 \right) \quad (8)$$

where $T_{i,t}$ is the temperature at station i and time t , and Δ_t^2 denotes the second-order temporal difference.

The final training objective combines these terms:

$$\mathcal{L} = \mathcal{L}_{\text{data}} + \lambda_1 \mathcal{L}_{\text{pw}} + \lambda_2 \mathcal{L}_{\text{smooth}} \quad (9)$$

where λ_1 and λ_2 are the weights of the physical terms.

4.4. Evaluation Metrics

Overall performance. Mean Absolute Error (MAE) and Mean Square Error (MSE) are used to evaluate the overall performance of the GSWF. MAE measures the predictive robustness of an algorithm but is insensitive to outliers, whereas MSE is sensitive to outliers and can amplify errors.

Metric for extreme value. In addition to standard metrics MAE and MSE, the precision in predicting extreme

Benchmarking Physics-Informed Time-Series Models for Operational Global Station Weather Forecasting

Table 3. Extreme weather events forecasting evaluation@SEDI (%) of NWP model and TSF-models. SEDI is calculated on the predicted results with 120 lengths. Note that the percentiles here include the lower bounds and upper bounds. Underline is the second-best performance.

Type	Methods	Temperature		Dewpoint		Wind Rate		Wind Direction		Sea Level Pressure	
		99.5th↑	90th↑	99.5th↑	90th↑	99.5th↑	90th↑	99.5th↑	90th↑	99.5th↑	90th↑
NWP (Operational)	ECMWF-HRES	37.4	82.6	35.4	76.4	10.2	40.8	13.1	45.4	77.5	89.7
Transformer-based	Informer	11.8	49.5	9.2	39.2	2.1	6.7	0.12	2.9	9.8	35.7
	Autoformer	12.4	52.1	8.3	38.9	0.3	7.8	0.13	1.6	10.4	32.1
	Pyraformer	10.7	54.8	7.2	40.1	0.6	7.2	0.06	1.1	10.5	26.2
	FEDformer	11.9	50.9	9.9	40.7	2.9	9.5	0.08	0.7	7.5	21.4
	PatchTST	10.9	50.8	8.9	42.4	0.5	8.9	0.10	2.2	13.5	36.7
	Corrformer	10.9	48.9	8.4	39.9	1.7	8.4	0.12	0.9	8.9	30.9
	iTransformer	14.1	55.0	10.4	44.8	1.3	10.3	0.14	2.3	15.9	37.5
MLP-based	STID	0.0	1.4	0.0	2.3	0.1	0.1	0.00	0.0	0.0	0.2
	DLinear	5.8	18.8	3.2	19.9	0.3	5.1	0.13	1.7	2.8	17.5
	SparseTSF	6.1	41.1	9.7	43.4	1.1	10.5	0.13	3.7	7.5	31.5
	TimeMixer	11.9	53.7	8.9	42.7	1.1	8.7	0.01	1.0	11.7	33.0
	WPMixer	11.9	53.1	8.2	42.3	0.8	8.4	0.01	1.0	10.6	33.1
GNN-based	MTGNN	3.1	9.9	2.9	9.0	0.1	4.0	0.08	0.5	1.1	3.9
LTMs	Chronos	26.2	59.5	16.9	47.1	6.3	18.0	2.51	9.6	18.7	41.3
	Timer	14.2	52.3	8.4	41.0	1.2	9.1	0.13	2.8	9.4	32.6
Physics-based	PhysicsFormer (Ours)	<u>30.6</u>	<u>77.7</u>	<u>20.4</u>	<u>61.6</u>	<u>7.8</u>	<u>28.0</u>	<u>5.01</u>	<u>21.2</u>	<u>62.6</u>	<u>66.0</u>

weather events, such as unusually high or low temperatures, is crucial in real-world applications. Hence, we introduce a specialized metric, the Symmetric Extremal Dependence Index (SEDI). (Han et al., 2024b; Xu et al., 2024). It classifies each prediction in its station location as either extreme or normal weather based on upper quantile thresholds (90%, 95%, 98%, and 99.5%) or lower quantile thresholds (10%, 5%, 2%, and 0.5%). The calculation of SEDI value can be formulated as:

$$\begin{aligned}
 \text{SEDI}(p) = & \frac{\sum(\hat{X} < Q_L^p \& X < Q_L^p)}{\sum(X < Q_L^p) + \sum(X > Q_U^p)} \\
 & + \frac{\sum(\hat{X} > Q_U^p \& X > Q_U^p)}{\sum(X < Q_L^p) + \sum(X > Q_U^p)}
 \end{aligned} \tag{10}$$

where $\hat{X} < Q_L^p$ and $X < Q_L^p$ judge whether the predicted or observed data point belongs to the extreme event or not based on the threshold Q_L^p , and vice versa for the upper percentiles. Here we access both two opposite percentiles for accessing extremely small values (e.g., winter storm) and extremely large values (e.g., heatwave). $\text{SEDI} \in [0, 1]$ quantifies the model’s ability to correctly identify extreme weather events. Higher SEDI indicates better performance in extreme weather prediction.

4.5. Experimental Protocols

Dataset splitting. The WEATHER-5K dataset is divided into training (2014–2021), validation (2022), and test (2023) subsets, following an 8:1:1 ratio.

Task settings. To enable fair comparison across baselines, we align the input length of all models. Each model predicts the τ -step future based on 48 historical steps, a choice informed by performance trends for four weather variables (Appendix Figure 8) and balancing computation with accuracy. We predict future weather conditions for lead times of 1, 3, 5, and 7 days, corresponding to 24-, 72-, 120-, and 168-step future data. Results are reported once, which suffices due to the dataset’s large volume and observed stability across different seeds.

Implementation details. Full implementation details, including training settings, hyperparameters, and hardware specifications, are provided in Appendix E.

4.6. Observations and Findings

RQ1: How do TSF models compare with NWP models in terms of general performance? Overall, as shown in Table 2, the NWP model, *i.e.*, ECMWF-HRES (EC), outperforms all existing TSF methods across nearly all variables, except for wind speed and direction. In Table 8 and 9 in the Appendix, we further analyze performance based on long-term prediction duration. Specifically, in short-term prediction (lead time = 24 hours), some TSF methods (e.g., Pyraformer (Liu et al., 2021)) exhibit comparable performance. However, for long-term prediction, cumulative error stabilizes and then increases significantly after the third day. This suggests that predictive errors become substantial beyond three days, indicating considerable room for improvement in long-term forecasting accuracy.

RQ2: Can TSF models effectively predict extreme

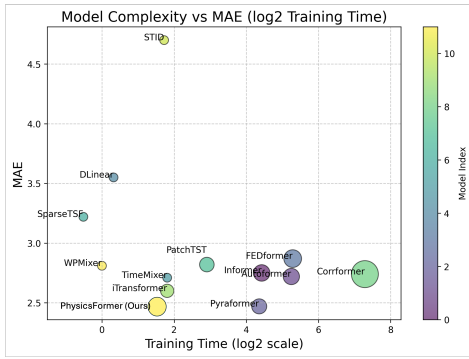


Figure 3. Model performance vs complexity. The bubble area represents the parameters in log2 scale.

weather events as an operational metric? Table 3 presents the predictive performance of various models on extreme values. Our analysis reveals that TSF models consistently fail to capture the lower and upper quantiles (90% and 99.5%), while numerical models excel at forecasting these extremes as a crucial capability for operational assessments of extreme weather events. Moreover, wind prediction shows the poorest performance among all variables, likely due to the non-stationary nature of wind distributions. These findings underscore the need for future research to enhance TSF models’ ability to capture extreme values for more robust operational forecasting.

RQ3: Are large-parameter TSF models necessary for weather forecasting? Figure 3 and Table 7 compare the model complexity and prediction accuracy (averaged over 72 hours) of various baselines. Our findings indicate that increasing parameter counts does not necessarily lead to better accuracy. For instance, Pyraformer (Liu et al., 2021) outperforms other models while using a relatively low number of parameters (7.54 MB) and lower training costs. In contrast, Timer (Liu et al., 2024d) and Corrformer (Wu et al., 2023), despite having much higher parameter counts (84 MB and 666 MB), offer little improvement or even worse performance. Although larger models like LTMs may excel in extreme event prediction (see Table 3), Chronos, with only half as many parameters (48 MB), outperforms Timer. Therefore, for practical deployment and frequent updates, smaller models may be more suitable for time series forecasting in weather applications.

RQ4: How does PhysicsFormer compare with existing TSF and NWP models? As shown in Table 2, PhysicsFormer outperforms all baseline TSF methods across most variables and matches or exceeds ECMWF-HRES (EC) in short- and medium-term forecasts. This stems from the dynamic core, providing physically-consistent baseline predictions, and the physics-informed residual learning, which lets the Transformer correct unresolved patterns while respecting meteorological laws. As Figure 3 shows, our approach achieves strong performance with relatively fewer param-

eters and training time, demonstrating that combining a physically-grounded core with a Transformer backbone and physics-informed loss yields accurate, physically-consistent forecasts efficiently.

RQ5: How to improve future weather forecasting methods leveraging the advantages of TSF and NWP models? Most NWP models (Bi et al., 2023; Lam et al., 2023; Han et al., 2024a) can provide robust global atmospheric forecasts. By utilizing outputs from these models, we can develop bias correction models tailored to meteorological stations. Leveraging this diverse information by bridging GSWF with numerical prediction models could potentially enhance weather prediction accuracy at these stations.

4.7. Case Study: Heatwave Forecasting

Here we evaluate the performance of several models in forecasting the 2022 summer heatwave in Chongqing. As shown in Figure 4, current time-series forecasting (TSF) methods, such as iTransformer and SparseTSF, still lag behind PhysicsFormer in capturing extreme weather events. PhysicsFormer achieves the lowest MAE (1.23), demonstrating superior accuracy. However, the Chronos model (MAE 1.82), leveraging large language model, shows significant potential by narrowing the gap with PhysicsFormer. These results highlight the need for further advancements in TSF methods to improve their effectiveness in extreme event predictions.

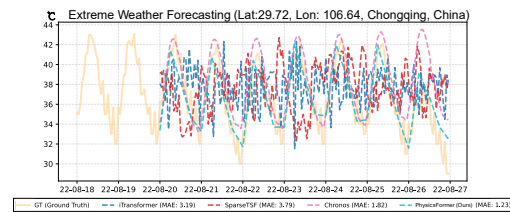


Figure 4. Comparison of extreme weather forecasting showcases using several models.

5. Conclusion

To ensure accurate, efficient, and scalable weather forecasting for global stations, we introduce WEATHER-5K as a new benchmark dataset. WEATHER-5K encompasses numerous global stations, providing comprehensive, long-term meteorological data. This dataset enables state-of-the-art time-series forecasting methods to be easily adopted and yield promising results. However, we also noticed that current methods might still lag behind numerical weather prediction models, particularly for longer lead times. We further propose a physics-informed model that integrates a dynamic core with physical-constraint losses, improving prediction accuracy. WEATHER-5K presents new challenges and opportunities, fostering innovative research.

6. Impact Statement

This work aims to advance the development of machine learning models for time-series forecasting in weather prediction. While the methods and dataset are intended to improve scientific understanding and forecasting accuracy. The dataset and models may benefit researchers and operational forecasting systems, contributing positively to weather prediction and disaster preparedness.

References

- Ecmwf-hres. URL <https://www.ecmwf.int/en/forecasts/documentation-and-support/changes-ecmwf-model>. Accessed: 2024-10-02.
- Integrated surface database. URL www.ncei.noaa.gov/products/land-based-station/integrated-surface-database. Accessed: 2024-10-02.
- Time-series-library. URL <https://github.com/thuml/Time-Series-Library>. Accessed: 2024-10-02.
- Achiam, J., Adler, S., Agarwal, S., Ahmad, L., Akkaya, I., Aleman, F. L., Almeida, D., Altenschmidt, J., Altman, S., Anadkat, S., et al. Gpt-4 technical report. *arXiv preprint arXiv:2303.08774*, 2023.
- Ansari, A. F., Stella, L., Turkmen, A. C., Zhang, X., Mercado, P., Shen, H., Shchur, O., Rangapuram, S. S., Arango, S. P., Kapoor, S., et al. Chronos: Learning the language of time series. *Transactions on Machine Learning Research*, 2024.
- Bai, L., Yao, L., Li, C., Wang, X., and Wang, C. Adaptive graph convolutional recurrent network for traffic forecasting. *Advances in neural information processing systems*, 33:17804–17815, 2020.
- Bi, K., Xie, L., Zhang, H., Chen, X., Gu, X., and Tian, Q. Accurate medium-range global weather forecasting with 3d neural networks. *Nature*, 619(7970):533–538, 2023.
- Challu, C., Olivares, K. G., Oreshkin, B. N., Ramirez, F. G., Canseco, M. M., and Dubrawski, A. Nhits: Neural hierarchical interpolation for time series forecasting. In *Proceedings of the AAAI Conference on Artificial Intelligence*, volume 37, pp. 6989–6997, 2023.
- Chen, K., Han, T., Gong, J., Bai, L., Ling, F., Luo, J.-J., Chen, X., Ma, L., Zhang, T., Su, R., et al. Fengwu: Pushing the skillful global medium-range weather forecast beyond 10 days lead. *arXiv preprint arXiv:2304.02948*, 2023.
- Gebru, T., Morgenstern, J., Vecchione, B., Vaughan, J. W., Wallach, H., Iii, H. D., and Crawford, K. Datasheets for datasets. *Communications of the ACM*, 64(12):86–92, 2021.
- Godahehwa, R., Bergmeir, C., Webb, G. I., Hyndman, R. J., and Montero-Manso, P. Monash time series forecasting archive. In *Neural Information Processing Systems Track on Datasets and Benchmarks*, 2021.
- Goswami, M., Szafer, K., Choudhry, A., Cai, Y., Li, S., and Dubrawski, A. Moment: A family of open time-series foundation models. In *International Conference on Machine Learning*, pp. 16115–16152. PMLR, 2024.
- Gu, A. and Dao, T. Mamba: Linear-time sequence modeling with selective state spaces. *arXiv preprint arXiv:2312.00752*, 2023.
- Han, H., Zhang, M., Hou, M., Zhang, F., Wang, Z., Chen, E., Wang, H., Ma, J., and Liu, Q. Stgcn: a spatial-temporal aware graph learning method for poi recommendation. In *2020 IEEE International Conference on Data Mining (ICDM)*, pp. 1052–1057. IEEE, 2020.
- Han, T., Guo, S., Ling, F., Chen, K., Gong, J., Luo, J., Gu, J., Dai, K., Ouyang, W., and Bai, L. Fengwu-ghr: Learning the kilometer-scale medium-range global weather forecasting. *arXiv preprint arXiv:2402.00059*, 2024a.
- Han, T., Guo, S., Xu, W., Bai, L., et al. Cra5: Extreme compression of era5 for portable global climate and weather research via an efficient variational transformer. *arXiv preprint arXiv:2405.03376*, 2024b.
- Hersbach, H., Bell, B., Berrisford, P., Biavati, G., Horányi, A., Muñoz Sabater, J., Nicolas, J., Peubey, C., Radu, R., Rozum, I., et al. Era5 hourly data on single levels from 1979 to present. *Copernicus climate change service (c3s) climate data store (cds)*, 10(10.24381), 2018.
- Jiao, D., Xu, N., Yang, F., and Xu, K. Evaluation of spatial-temporal variation performance of era5 precipitation data in china. *Scientific Reports*, 11(1):17956, 2021.
- Jin, M., Wang, S., Ma, L., Chu, Z., Zhang, J. Y., Shi, X., Chen, P.-Y., Liang, Y., Li, Y.-F., Pan, S., et al. Time-llm: Time series forecasting by reprogramming large language models. *arXiv preprint arXiv:2310.01728*, 2023.
- Lai, G., Chang, W.-C., Yang, Y., and Liu, H. Modeling long-and short-term temporal patterns with deep neural networks. In *The 41st international ACM SIGIR conference on research & development in information retrieval*, pp. 95–104, 2018.

- Lam, R., Sanchez-Gonzalez, A., Willson, M., Wirnsberger, P., Fortunato, M., Alet, F., Ravuri, S., Ewalds, T., Eaton-Rosen, Z., Hu, W., et al. Learning skillful medium-range global weather forecasting. *Science*, 382(6677):1416–1421, 2023.
- Li, F., Feng, J., Yan, H., Jin, G., Yang, F., Sun, F., Jin, D., and Li, Y. Dynamic graph convolutional recurrent network for traffic prediction: Benchmark and solution. *ACM Transactions on Knowledge Discovery from Data*, 17(1):1–21, 2023.
- Li, Y., Yu, R., Shahabi, C., and Liu, Y. Diffusion convolutional recurrent neural network: Data-driven traffic forecasting. In *International Conference on Learning Representations*, 2018.
- Li, Y., Lu, X., Wang, Y., and Dou, D. Generative time series forecasting with diffusion, denoise, and disentanglement. *Advances in Neural Information Processing Systems*, 35: 23009–23022, 2022.
- Liang, Y., Wen, H., Nie, Y., Jiang, Y., Jin, M., Song, D., Pan, S., and Wen, Q. Foundation models for time series analysis: A tutorial and survey. In *Proceedings of the 30th ACM SIGKDD conference on knowledge discovery and data mining*, pp. 6555–6565, 2024.
- Lin, S., Lin, W., Wu, W., Chen, H., and Yang, J. Sparsesf: Modeling long-term time series forecasting with* 1k* parameters. In *International Conference on Machine Learning*, pp. 30211–30226. PMLR, 2024.
- Liu, S., Yu, H., Liao, C., Li, J., Lin, W., Liu, A. X., and Dustdar, S. Pyraformer: Low-complexity pyramidal attention for long-range time series modeling and forecasting. In *International conference on learning representations*, 2021.
- Liu, X., Xia, Y., Liang, Y., Hu, J., Wang, Y., Bai, L., Huang, C., Liu, Z., Hooi, B., and Zimmermann, R. Largest: A benchmark dataset for large-scale traffic forecasting. *Advances in Neural Information Processing Systems*, 36, 2024a.
- Liu, Y., Hu, T., Zhang, H., Wu, H., Wang, S., Ma, L., and Long, M. itransformer: Inverted transformers are effective for time series forecasting. 2024b.
- Liu, Y., Qin, G., Huang, X., Wang, J., and Long, M. Autotimes: Autoregressive time series forecasters via large language models. *arXiv preprint arXiv:2402.02370*, 2024c.
- Liu, Y., Zhang, H., Li, C., Huang, X., Wang, J., and Long, M. Timer: Transformers for time series analysis at scale. *arXiv e-prints*, pp. arXiv–2402, 2024d.
- Lynch, P. The origins of computer weather prediction and climate modeling. *Journal of computational physics*, 227(7):3431–3444, 2008.
- Murad, M. M. N., Aktukmak, M., and Yilmaz, Y. Wp-mixer: Efficient multi-resolution mixing for long-term time series forecasting. *arXiv preprint arXiv:2412.17176*, 2024.
- Nagda, M., Abijuru, J., Ostheimer, P., Kloft, M., and Fellenz, S. Piano: Physics informed autoregressive network. *arXiv preprint arXiv:2508.16235*, 2025.
- Nasiri, M., Kortelainen, J., and Särkkä, S. Dual-level models for physics-informed multi-step time series forecasting. *arXiv preprint arXiv:2601.07640*, 2026.
- Nie, Y., Nguyen, N. H., Sinthong, P., and Kalagnanam, J. A time series is worth 64 words: Long-term forecasting with transformers. In *The Eleventh International Conference on Learning Representations*, 2023.
- Oreshkin, B. N., Carпов, D., Chapados, N., and Bengio, Y. N-beats: Neural basis expansion analysis for interpretable time series forecasting. *arXiv preprint arXiv:1905.10437*, 2019.
- Phillips, N. A. The general circulation of the atmosphere: A numerical experiment. *Quarterly Journal of the Royal Meteorological Society*, 82(352):123–164, 1956.
- Raffel, C., Shazeer, N., Roberts, A., Lee, K., Narang, S., Matena, M., Zhou, Y., Li, W., and Liu, P. J. Exploring the limits of transfer learning with a unified text-to-text transformer. *Journal of machine learning research*, 21(140):1–67, 2020.
- Schuhmann, C., Beaumont, R., Vencu, R., Gordon, C., Wightman, R., Cherti, M., Coombes, T., Katta, A., Mullis, C., Wortsman, M., et al. Laion-5b: An open large-scale dataset for training next generation image-text models. *Advances in Neural Information Processing Systems*, 35: 25278–25294, 2022.
- Sel, K., Mohammadi, A., Pettigrew, R. I., and Jafari, R. Physics-informed neural networks for modeling physiological time series for cuffless blood pressure estimation. *npj Digital Medicine*, 6(1):110, 2023.
- Shao, Z., Zhang, Z., Wang, F., Wei, W., and Xu, Y. Spatial-temporal identity: A simple yet effective baseline for multivariate time series forecasting. In *Proceedings of the 31st ACM international conference on information & knowledge management*, pp. 4454–4458, 2022.
- Trindade, A. ElectricityLoadDiagrams20112014. UCI Machine Learning Repository, 2015. DOI: <https://doi.org/10.24432/C58C86>.

- Vaswani, A., Shazeer, N., Parmar, N., Uszkoreit, J., Jones, L., Gomez, A. N., Kaiser, Ł., and Polosukhin, I. Attention is all you need. *Advances in neural information processing systems*, 30, 2017.
- Wang, S., Wu, H., Shi, X., Hu, T., Luo, H., Ma, L., Zhang, J. Y., and Zhou, J. Timemixer: Decomposable multiscale mixing for time series forecasting. 2024.
- Wu, H., Xu, J., Wang, J., and Long, M. Autoformer: Decomposition transformers with auto-correlation for long-term series forecasting. *Advances in neural information processing systems*, 34:22419–22430, 2021.
- Wu, H., Zhou, H., Long, M., and Wang, J. Interpretable weather forecasting for worldwide stations with a unified deep model. *Nature Machine Intelligence*, 5(6):602–611, 2023.
- Wu, Z., Pan, S., Long, G., Jiang, J., Chang, X., and Zhang, C. Connecting the dots: Multivariate time series forecasting with graph neural networks. In *Proceedings of the 26th ACM SIGKDD international conference on knowledge discovery & data mining*, pp. 753–763, 2020.
- Xu, W., Chen, K., Han, T., Chen, H., Ouyang, W., and Bai, L. Extremecast: Boosting extreme value prediction for global weather forecast. *arXiv preprint arXiv:2402.01295*, 2024.
- Xu, Y. and Fu, Y. Sports-traj: A unified trajectory generation model for multi-agent movement in sports. *arXiv preprint arXiv:2405.17680*, 2024.
- Xue, H. and Salim, F. D. Promptcast: A new prompt-based learning paradigm for time series forecasting. *IEEE Transactions on Knowledge and Data Engineering*, 36(11):6851–6864, 2023.
- Yang, S., Liu, Z., Shi, Z., and Zou, Z. Wssm: Geographic-enhanced hierarchical state-space model for global station weather forecast. *arXiv preprint arXiv:2501.11238*, 2025a.
- Yang, S., Shi, Z., and Zou, Z. Unified multi-agent trajectory modeling with masked trajectory diffusion. In *Proceedings of the IEEE/CVF International Conference on Computer Vision*, pp. 27563–27574, 2025b.
- Zeng, A., Chen, M., Zhang, L., and Xu, Q. Are transformers effective for time series forecasting? In *Proceedings of the AAAI conference on artificial intelligence*, volume 37, pp. 11121–11128, 2023.
- Zhou, H., Zhang, S., Peng, J., Zhang, S., Li, J., Xiong, H., and Zhang, W. Informer: Beyond efficient transformer for long sequence time-series forecasting. In *Proceedings of the AAAI conference on artificial intelligence*, volume 35, pp. 11106–11115, 2021.
- Zhou, T., Ma, Z., Wen, Q., Wang, X., Sun, L., and Jin, R. Fedformer: Frequency enhanced decomposed transformer for long-term series forecasting. In *International conference on machine learning*, pp. 27268–27286. PMLR, 2022.
- Zhou, T., Niu, P., Sun, L., Jin, R., et al. One fits all: Power general time series analysis by pretrained lm. *Advances in neural information processing systems*, 36:43322–43355, 2023.

A. Limitation.

Spatial Quality. The current version of WEATHER-5K offers observations from a global network, but coverage remains sparse in regions like Africa and South America. Future enhancements will focus on integrating data from diverse sources, such as MADIS reports (including METER and Mesonet), to achieve denser station distribution and improve evaluation accuracy.

Missing Data Handling. To maintain data integrity, we utilized interpolated results from the ERA5 dataset to fill in missing observations. While this interpolation introduces some errors, minimally affecting temperature, dew point temperature, and pressure but significantly impacting wind data, we ensured that only a small fraction of missing values were filled in to minimize these errors.

B. Observations and Future Directions

After a comprehensive evaluation, our benchmark reveals that current TSF methods lag behind operational NWP models, particularly in long-term forecasting and extreme event prediction as shown in Figure 1. To bridge these gaps, we identify several critical future directions for advancing TSF research for operational weather forecasting, based on insights from our dataset and benchmarks:

- Improve overall weather forecasting performance by prioritizing *long-term forecast* accuracy.
- Address the significant limitations in predicting *extreme weather events* by focusing research on this critical area.
- Our benchmarks indicate that **larger** models with more parameters *do not* consistently yield better performance; developing lightweight, efficient TSF models may be more beneficial.
- Some metrics (*e.g.*, wind rate) suggest that TSF can outperform NWP. A *hybrid forecasting model* that enjoys the simplicity of TSF with the operational strengths of NWP may offer a promising solution.

In summary, our work provides valuable resources, benchmarks, and guidance to propel TSF research in weather forecasting. We believe it will enable researchers to better evaluate and compare algorithms, fostering the development of more accurate and reliable forecasting techniques for global weather systems.

C. Dataset Documentation

We organize the dataset documentation based on the template of datasheets for datasets (Gebu et al., 2021).

C.1. Motivation

For what purpose was the dataset created? Was there a specific task in mind? Was there a specific gap that needed to be filled? Please provide a description.

This dataset is created with the following motivations: 1) The current weather station dataset limits the applicability of forecasting models in real-world scenarios. Hence, it is urgent to develop a comprehensive global station weather dataset that enables forecasting models to generalize across diverse stations and regions worldwide. 2) The limited sizes of existing time-series datasets may not reflect the real performance of the forecasting models, the proposed large weather station dataset can also serve as an extensive time-series dataset to perform comprehensive time-series forecasting benchmarks for various forecasting methods. 3) The existing simple datasets fail to encompass the complex scientific problems that researchers need to discover and resolve, thereby hindering progress in the field of time-series prediction. The proposed dataset offers a diverse temporal and spatial range of time-series data, enabling a comprehensive evaluation of time-series forecasting methods and driving significant advancements in the field. 4) A large-scale weather station dataset is a crucial source of observational data for numerical weather prediction models, effectively bridging the gap between numerical models and station-based predictions. This not only improves the accuracy of numerical forecasts but also plays a vital role in verifying and evaluating the predictive performance of numerical weather prediction models.

C.2. Composition

What do the instances that comprise the dataset represent (e.g., documents, photos, people, countries)? Are there multiple types of instances (e.g., movies, users, and ratings; people and interactions between them; nodes and edges)? Please provide a description.

WEATHER-5K consists of 5,672 CSV files. Each CSV file represents data from a single weather station, with hourly observations recorded from 2014 to 2023. The dataset represents a collection of weather observation data, where each instance corresponds to an hourly observation from a specific weather station, with various meteorological measurements and auxiliary information.

How many instances are there in total (of each type, if appropriate)?

WEATHER-5K has a total number of 5,762 stations with a 10-year time coverage and includes 8 mandatory variables and 2 auxiliary features. For each sensor. It also possesses 87,648 instances.

Does the dataset contain all possible instances or is it a sample (not necessarily random) of instances from a larger set? If the dataset is a sample, then what is the larger set? Is the sample representative of the larger set (e.g., geographic coverage)? If so, please describe how this representativeness was validated/verified.

Our dataset is collected and further processed using data sourced from the National Centers for Environmental Information (NCEI), specifically the Integrated Surface Database (ISD),². Although the ISD contains records from over 20,000 stations spanning several decades, not all stations are suitable for machine learning applications. For instance, some stations are no longer operational, many do not report data on an hourly basis, and numerous stations have missing values for critical weather elements. To get a high-quality weather station dataset, a meticulous selection process was conducted to include only long-term, hourly reporting stations that are currently operational and provide essential observations such as temperature, dew point temperature, wind, and sea level pressure. After that, we use the process procedure detailed in Section 3 to make the final WEATHER-5K, which is in the principle of applicability for time-series forecasting research.

What data does each instance consist of? “Raw” data (e.g., unprocessed text or images) or features? In either case, please provide a description.

The key characteristics of each instance are:

1. **Instance Type:** Each row in the CSV file represents a single hourly weather observation from a specific weather station.
2. **Instance Fields:** Each instance (row) contains the fields as detailed in Table 4.
3. **Temporal Dimension:** The dataset covers hourly weather observations from 2014-01-01 T00:00:00 to 2023-12-31 T00:00:00, a total of 87,648 time slots.
4. **Spatial Dimension:** Each CSV file represents data from a single weather station, identified by its geographic coordinates (LONGITUDE and LATITUDE).

Table 4. Instance Fields.

Field	Description
DATE	The date of the observation
LONGITUDE	The longitude of the weather station
LATITUDE	The latitude of the weather station
TMP	The temperature observation
DEW	The dew point observation
WND_ANGLE	The wind angle observation
WND_RATE	The wind rate observation
SLP	The sea level pressure observation
MASK	A binary list indicate the quality of the observation
TIME_DIFF	An auxiliary field

²www.ncei.noaa.gov/products/land-based-station/integrated-surface-database

Is there a label or target associated with each instance? If so, please provide a description.

No, weather observation data can take itself as label in the forecasting task, and weather forecasting can be considered as a self-supervised learning task.

Is any information missing from individual instances? If so, please provide a description, explaining why this information is missing (e.g., because it was unavailable).

No, many efforts have been made to ensure there is no missing data in the WEATHER-5K dataset.

Are relationships between individual instances made explicit (e.g., users' movie ratings, social network links)? If so, please describe how these relationships are made explicit.

Yes, the weather stations in the dataset have geographical relationships, and we have used latitude, longitude, and elevation to represent their geographic locations. This information can be leveraged in subsequent work to model the spatial relationships between the instances.

Are there recommended data splits (e.g., training, development/validation, testing)? If so, please provide a description of these splits, explaining the rationale behind them.

Yes, we chronologically split the data into train (2013-01-01 to 2021-12-31), validation (2022-01-01 to 2022-12-31), and test (2023-01-01 to 2023-12-31) sets, with a ratio of 8:1:1.

Are there any errors, sources of noise, or redundancies in the dataset? If so, please provide a description.

Yes, the errors and noise in the dataset arise from two main sources. Firstly, the use of meteorological automatic stations introduces a certain degree of observational error, particularly in the measurement of wind speed and direction, which are relatively difficult to measure accurately. Secondly, in our data processing efforts to ensure the completeness of the dataset, we have employed interpolation operations, which can introduce some additional error. However, the proportion of error introduced by the interpolation is relatively small.

Is the dataset self-contained, or does it link to or otherwise rely on external resources (e.g., websites, tweets, other datasets)?

Yes, it is self-contained.

Does the dataset contain data that might be considered confidential (e.g., data that is protected by legal privilege or by doctor-patient confidentiality, data that includes the content of individuals' non-public communications)? If so, please provide a description.

No, all our data are from a publicly available data source, i.e., NCEI.

Does the dataset contain data that, if viewed directly, might be offensive, insulting, threatening, or might otherwise cause anxiety? If so, please describe why.

No, all our data are numerical.

C.3. Collection Process

How was the data associated with each instance acquired? Was the data directly observable (e.g., raw text, movie ratings), reported by subjects (e.g., survey responses), or indirectly inferred/derived from other data (e.g., part-of-speech tags, model-based guesses for age or language)?

We source the data from the the Integrated Surface Database (ISD) oginized and maintained by the National Centers for Environmental Information (NCEI). ISD is a global database that consists of hourly and synoptic surface observations compiled from numerous sources into a single common ASCII format and common data model. ISD integrates data from more than 100 original data sources.

What mechanisms or procedures were used to collect the data (e.g., hardware apparatuses or sensors, manual human curation, software programs, software APIs)? How were these mechanisms or procedures validated?

NCEI (formerly the National Climatic Data Center) started developing ISD in 1998 with assistance from partners in the U.S. Air Force and Navy, as well external funding from several sources. The database incorporates data from over 35,000 stations

around the world, with some that include having, and includes observations data from as far back as 1901. The number of stations with data in ISD increased substantially in the 1940s and again in the early 1970s. There are currently more than 14,000 active ISD stations that are updated daily in the database. The total uncompressed data volume is around 600 gigabytes; however, it continues to grow as more data are added.

If the dataset is a sample from a larger set, what was the sampling strategy (e.g., deterministic, probabilistic with specific sampling probabilities)?

The sampling strategy is deterministic.

Who was involved in the data collection process (e.g., students, crowdworkers, contractors) and how were they compensated (e.g., how much were crowdworkers paid)?

Our code collects publicly available data, which is free. On our side, we developed a download API to efficiently retrieve the source data, which was done by our team members.

Over what timeframe was the data collected? Does this timeframe match the creation timeframe of the data associated with the instances (e.g., recent crawl of old news articles)? If not, please describe the timeframe in which the data associated with the instances was created.

The WEATHER-5K dataset is collected and processed in 2024. This timeframe of the source data data is matches the creation timeframe of the data.

Were any ethical review processes conducted (e.g., by an institutional review board)?

No, such processes are unnecessary in our case.

C.4. Preprocessing/cleaning/labeling

Was any preprocessing/cleaning/labeling of the data done (e.g., discretization or bucketing, tokenization, part-of-speech tagging, SIFT feature extraction, removal of instances, processing of missing values)? If so, please provide a description.

Yes, to obtain a high-quality dataset of weather stations, a series of post-processing steps were performed on the raw weather station data collected from 2014 to 2024. Initially, 10,701 commonly operating stations were identified. The first step involved selecting stations that reported data every hour on the hour. However, many stations did not meet this criterion. To address this, a replacement method estimated missing hourly data points using the nearest available time points within a 30-minute window, significantly improving the distribution of valid hourly data. Some following processing steps are described in Section 3.

Was the “raw” data saved in addition to the preprocessed / cleaned/ labeled data (e.g., to support unanticipated future uses)? If so, please provide a link or other access point to the “raw” data.

The raw data are available in the NCEI. The link is: www.ncei.noaa.gov/products/land-based-station/integrated-surface-database. To get the preprocessed data, you can run the ‘weather_station_api.py’ in our final released repository.

Is the software that was used to preprocess/clean/label the data available? If so, please provide a link or other access point.

No.

C.5. Uses

Has the dataset been used for any tasks already? If so, please provide a description.

The dataset is used in this paper for the global station weather forecasting task.

Is there a repository that links to any or all papers or systems that use the dataset? If so, please provide a link or other access point.

No, but we may include a leader board and list papers using this dataset in the future.

What (other) tasks could the dataset be used for?

Weather data imputation, numerical weather prediction, and data assimilation

Is there anything about the composition of the dataset or the way it was collected and preprocessed/cleaned/labeled that might impact future uses?

We believe that our dataset will not encounter usage limit.

Are there tasks for which the dataset should not be used? If so, please provide a description.

No, users could use our dataset in any task as long as it does not violate laws.

C.6. Distribution

Will the dataset be distributed to third parties outside of the entity (e.g., company, institution, organization) on behalf of which the dataset was created? If so, please provide a description.

No, it will always be held on GitHub.

How will the dataset will be distributed (e.g., tarball on website, API, GitHub)? Does the dataset have a digital object identifier (DOI)?

The instructions for building WEATHER-5K will be available in the released code. The dataset does not have a digital object identifier currently.

When will the dataset be distributed?

On June 07, 2024.

Will the dataset be distributed under a copyright or other intellectual property (IP) license, and/or under applicable terms of use (ToU)? If so, please describe this license and/or ToU, and provide a link or other access point to.

Our benchmark dataset is released under a CC BY-NC 4.0 International License: <https://creativecommons.org/licenses/by-nc/4.0>. Our code implementation is released under the MIT License: <https://opensource.org/licenses/MIT>.

Have any third parties imposed IP-based or other restrictions on the data associated with the instances? If so, please describe these restrictions, and provide a link or other access point to, or otherwise reproduce, any relevant licensing terms, as well as any fees associated with these restrictions.

Yes, for commercial use, please check the website: <https://www.ncei.noaa.gov/>.

Do any export controls or other regulatory restrictions apply to the dataset or to individual instances? If so, please describe these restrictions, and provide a link or other access point to, or otherwise reproduce, any supporting documentation. No.

C.7. Maintenance

Who will be supporting/hosting/maintaining the dataset?

The authors of the paper.

Is there an erratum? If so, please provide a link or other access point.

Users can use GitHub to report issues or bugs.

Will the dataset be updated (e.g., to correct labeling errors, add new instances, delete instances)? If so, please describe how often, by whom, and how updates will be communicated to dataset consumers (e.g., mailing list, GitHub)?

Yes, the authors will actively update the code and data on GitHub. Any updates of the dataset will be announced in our GitHub repository.

If the dataset relates to people, are there applicable limits on the retention of the data associated with the instances (e.g., were the individuals in question told that their data would be retained for a fixed period of time and then

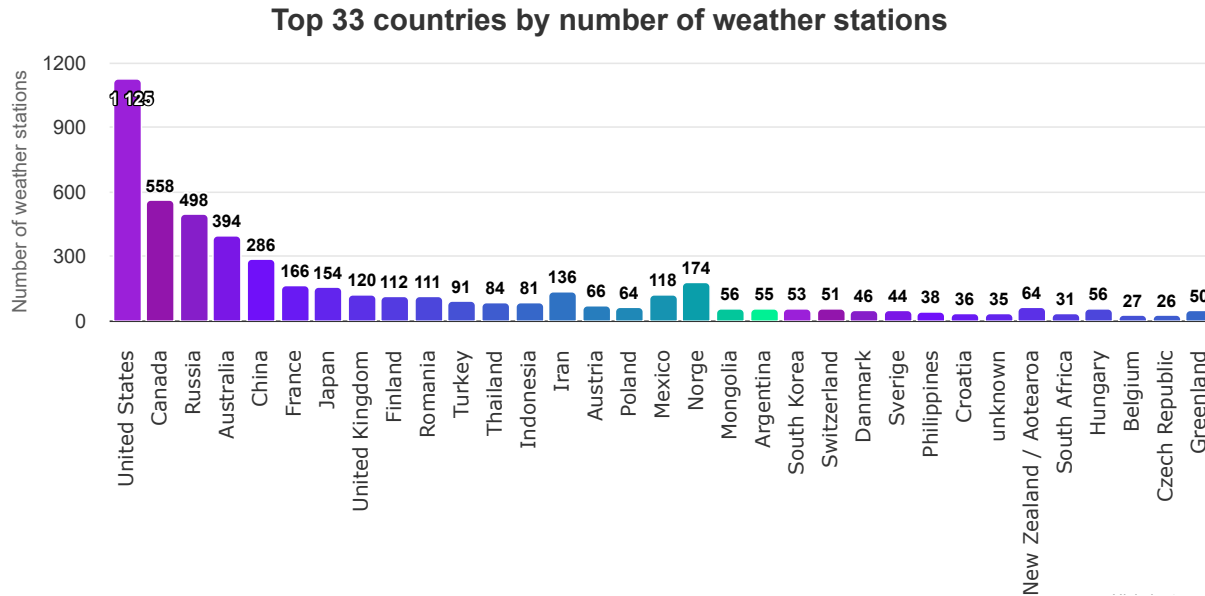


Figure 5. Statistics on the Number of Weather Stations in Different Countries and Regions.

deleted)? If so, please describe these limits and explain how they will be enforced.

The dataset does not relate to people.

Will older versions of the dataset continue to be supported/ hosted/ maintained? If so, please describe how. If not, please describe how its obsolescence will be communicated to dataset consumers.

Yes, we will provide the information on GitHub.

If others want to extend/augment/build on/contribute to the dataset, is there a mechanism for them to do so? If so, please provide a description. Will these contributions be validated/verified? If so, please describe how. If not, why not? Is there a process for communicating/distributing these contributions to dataset consumers? If so, please provide a description.

Yes, we welcome users to submit pull requests on GitHub, and we will actively validate the requests.

D. More Dataset Analysis

Disparities of station density. The WEATHER-5K dataset reveals regional disparities in the distribution of weather stations, which can significantly impact the learning and understanding of atmospheric dynamics in certain areas. As illustrated in Figure 6 a), some land regions have sparse data coverage compared to others. These disparities can be attributed to factors such as geographical characteristics, levels of economic development, and the strategic placement of weather stations. Note that the number of oceanic stations is also very limited due to the expensive cost of establishing stations at sea. Addressing these disparities and expanding coverage in underrepresented areas is crucial for improving the accuracy and reliability of weather forecasting and analysis in those regions.

Different data patterns. By visualizing the temperature observations, as shown in Figure 6 b), *temperature* shows a seasonal pattern. However, wind speeds are non-stationary, characterized by intense fluctuations and a lack of clear patterns, making them challenging to predict.

Compare WEATHER-5K with ERA5. ERA5 is a simulated dataset, not based on in-situ observations, which limits its applicability in real-world scenarios. In contrast, the WEATHER-5K dataset is derived from in-situ observations. To illustrate their differences, we calculate the RMSE of ERA5 against in-situ observations (Jiao et al., 2021), as shown in Figure 6 e), which presents the overall RMSE when comparing ERA5 data to real-world observations, underscoring the importance of building a weather dataset using actual observations. In addition to the point-based comparison, Figure 6 c) and Figure 6 f) also demonstrate the relevance and difference between the reanalysis data and observations.

Benchmarking Physics-Informed Time-Series Models for Operational Global Station Weather Forecasting

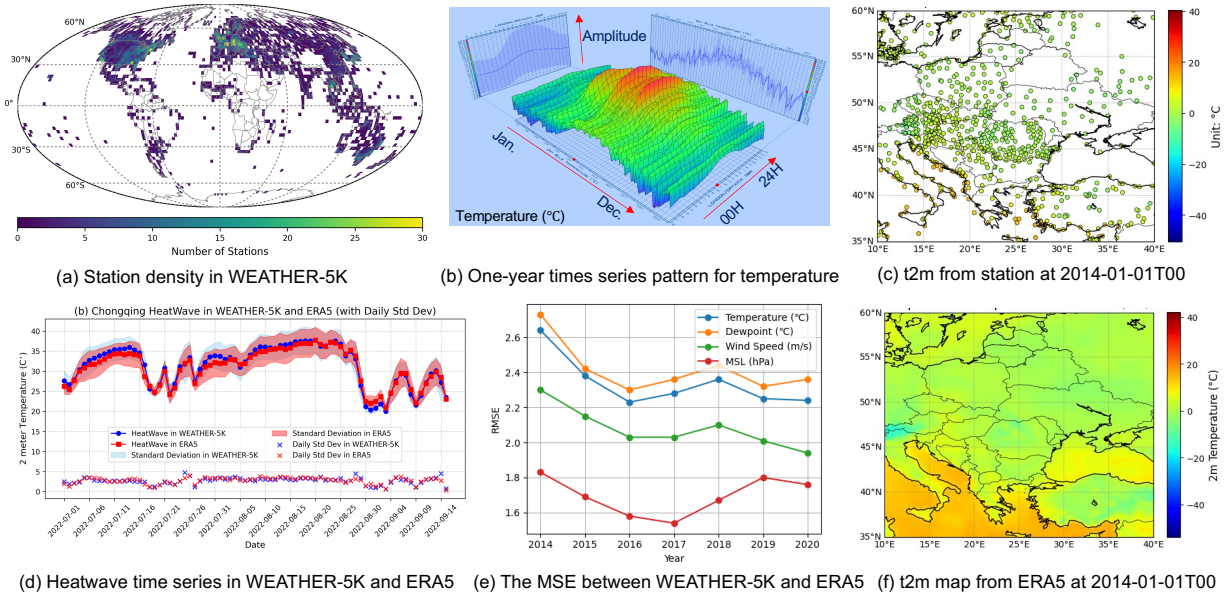


Figure 6. Data analysis and visualizations. In figure (d), The daily 2m temperature at station 57516099999 from 1st July to 15th September, in 2022, where filled areas represent the variance from the daily mean.

Heatwave analysis in China, 2022. Figure 6 d) presents the daily temperature variations in Chongqing city, China (ID: 57516099999) from July to September 2022. It shows that both the average and maximum temperatures of WEATHER-5K exceed those of ERA5 on most heatwave days, indicating that ERA5 underestimated the diurnal temperature range at this station during the heatwave period. Although only one station is showcased here, it is widely recognized that ERA5 cannot accurately capture extreme events (Bi et al., 2023).

Station distribution by countries. Figure 5 shows the histogram of the number of weather stations in the WEATHER-5K dataset over 33 countries. WEATHER-5K is a global database, though the best spatial coverage is evident in North America, Europe, Australia, and parts of Asia. Coverage in the Northern Hemisphere is better than the Southern Hemisphere.

Compare ISD with MADIS Data Source. Overall, as shown in Table 5, ISD is more diverse and offers broader coverage. Specifically, the surface data in MADIS mainly includes METER³ and Mesonet⁴. Its reports primarily come from the U.S. while ISD collects surface weather data from more than 35,000 stations worldwide. Additionally, ISD spans a longer period from ‘1901 to the present’ and is fully public for users. In future research, we believe including MADIS for station-based weather forecasting will further enhance this field.

Table 5. Differences between ISD (database of WEATHER-5K) and MADIS

Dataset	Availability	Data Source	Time	Coverage
MADIS (METER and Mesonet)	Restricted	ASOS, AWOS, Airport Reports, CWOP, FAWH, GPSMet, KSDOT, RAWs, UDFCD, GLDNWS, IADOT, INTERNET	2001-present	Primarily in U.S.
ISD	Fully public	More than 100 original data sources	1901-present	35,000 global stations

Characteristics of data distribution. Figure 7 provides violin plots for several variables. For temperature and dewpoint, the distributions of their data have similar shapes. The upper and lower distributions of the data are symmetrical around the

³https://madis.ncep.noaa.gov/madis_metar.shtml

⁴https://madis.ncep.noaa.gov/madis_mesonet.shtml

Table 6. Statistics of WEATHER-5K dataset.

	Temperature	Dewpoint	Wind Direction	Wind Speed	Sea Level Pressure
Mean	12.71	6.53	191.19	3.37	1014.85
Standard Deviation	13.08	12.14	99.67	2.66	9.17

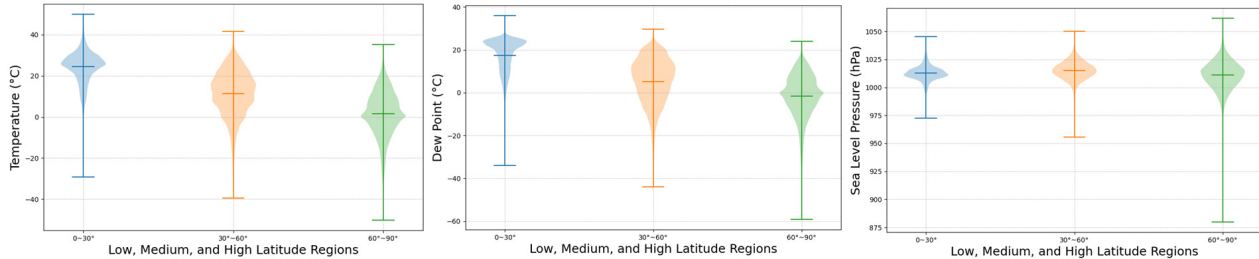


Figure 7. The violin plots of the temperature, dewpoint, and sea level pressure observations in the low, middle, and high latitudes, respectively categorized by these two features.

median. The temperature distribution is most concentrated in the low-latitude regions. As the latitude increases, the center of the temperature distribution starts to shift and also becomes more dispersed. This indicates that the temperature difference is larger in the mid-to-high latitude regions. For sea level pressure, we find that the distribution centers are similar across different latitudes, with little shift. However, as the latitude increases, the dispersion of sea level pressure becomes greater.

Climate mean and standard deviation. Table 6 presents the mean and standard deviation values for five key weather variables measured at 5,762 weather stations. The variables included are temperature, dewpoint, wind direction, wind speed, and sea level pressure. The mean temperature across the weather stations is 12.71 degrees, with a standard deviation of 13.08 degrees. For dewpoint, the mean is 6.53 degrees and the standard deviation is 12.14 degrees. The mean wind direction is 191.19 degrees, with a standard deviation of 99.67 degrees. The mean wind speed is 3.37 meters per second, with a standard deviation of 2.66 meters per second. Finally, the mean sea level pressure is 1014.85 millibars, with a standard deviation of 9.17 millibars. These statistics provide a high-level overview of the typical weather conditions captured by the network of weather stations.

Table 7. Efficiency comparisons. Statistics are tested based on the following setting: batch size →1024 in general except 5600 for Corrformer, MTGNN and STID, train time→estimated training time (in hours) for 300,000 iterations. task setting→48 input length and 120 output length. Hardware→224 Intel(R) Xeon(R) Platinum 8480CL CPUs @ 3.80 GHz, 2.0 TB RAM computing server, equipped with 8 NVIDIA H800 GPUs. Each experiment is conducted on a single GPU. Note that the total training time is also influenced by data read speed as some methods may suffer input starvation.

	Informer	Autoformer	Pyraformer	FEDformer	DLinear	TimeMixer
Training Time (Hours)	21~22	36~40	20 ~ 21	38 ~ 40	1.0 ~ 1.5	3.5
GPU Memory (MiB)	12,880	64,688	33,750	18,804	850	1,191
Parameters (M)	11.32	10.53	7.54	16.29	0.01	0.06
	PatchTST	Corrformer	iTransformer	MTGNN	STID	WPMixer
Training Time (Hours)	7~8	144~168	3~4	35	3.3	1
GPU Memory (MiB)	22,512	46,486	45,672	5,155	813	1,499
Parameters (M)	6.65	666.12	4.8	40.06	0.24	0.05
	SparseTSF	Timer	Chronos	PhysicsFormer (Ours)		
Training Time (Hours)	0.7	/	/	3		
GPU Memory (MiB)	525	/	/	9318		
Parameters (M)	0.0002	84	48	19.33		

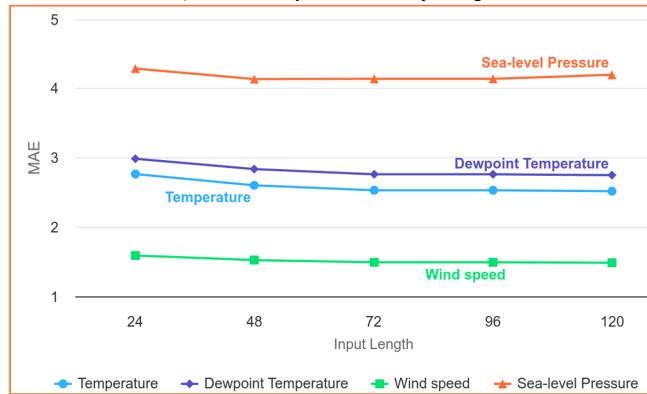


Figure 8. Ablation study on input length.

E. Implementation details and More Experimental Results

Implementation details. We develop and implement the baselines based on the Time-Series-Library (Tim). The training is performed for a total of 300,000 iterations, starting with a learning rate of $1e-4$. We employ the cosine decay strategy and gradually decay the learning rate to 0 by the end of training. The batch size for all models is set to 1,024, except for Corrformer, STID and MTGNN. During the validation phase, an early stopping is executed if training loss does not decrease for three consecutive times. The checkpoint with the lowest validation loss encountered prior to the early stop is saved and used for testing. Experiments are conducted on 224 Intel(R) Xeon(R) Platinum 8480CL CPUs @ 3.80 GHz, 2.0 TB RAM computing server, equipped with 8 NVIDIA H800 GPUs.

Full Benchmark Result. We present the full forecasting metrics for all methods at four different prediction lengths in Table 8 and Table 9. We also include methods (WSSM (Yang et al., 2025a)) based on Mamba and time series generation methods (UniMTD (Yang et al., 2025b), UniTraj (Xu & Fu, 2024)) in the table.

Ablation study. The ablation experiments are conducted to explore the impact of different input lengths on predictions. Here, we utilized the iTransformer (Liu et al., 2024b) model for verification. Specifically, we set the input length to 24, 48, 72, 96, and 120, while keeping the predicted length constant at 72. The experimental results are shown in Figure 8, illustrating the performance variation of MAE for four weather variables as the input sequence length increases. The results demonstrate that the performance for some variables (temperature and wind) is slightly improved when increasing the input length. On the other hand, the MAE error for sea level pressure rises slightly. We ultimately set the input length as 48 to balance computation and performance.

Efficiency comparisons. We summarize the efficiency comparisons in Table 7 details the complexity metrics, with LTMs employing zero-shot prediction.

Visualization results. In Figures 9, 10, 11, 12, 13, 14, 15, 16, 17, 18, 19, 20, we have plot visualization results to showcase the performance of various time-series forecasting methods, including Pyraformer, FEDformer, DLinear, PatchTST, iTransformer, Corrformer, STID, SparseTSF, TimeMixer, Chronos, Timer, and PhysicsFormer (our method). These visualizations provide a comparative analysis of how each of these different forecasting approaches performs on the time-series data.

By presenting the results in this series of figures, we are able to illustrate the unique characteristics and capabilities of each method. This allows the reader to gain a better understanding of the strengths and weaknesses of the various techniques, and how they may be suited for different types of time-series forecasting problems.

Benchmarking Physics-Informed Time-Series Models for Operational Global Station Weather Forecasting

Table 8. Full results of all the baseline models. (Part I)

Methods	Lead Time	Temperature		Dewpoint		Wind Rate		Wind Direc.		Sea Level Pressure	
		MAE	MSE	MAE	MSE	MAE	MSE	MAE	MSE	MAE	MSE
ECMWF-HRES	24	1.76	7.39	1.85	7.94	1.48	4.53	63.8	7158.3	0.86	2.68
	72	1.87	8.01	1.94	8.48	1.52	4.76	72.4	8215.6	1.06	3.31
	120	1.99	8.79	2.14	10.87	1.58	5.11	75.4	8647.7	1.38	5.15
	168	2.15	10.06	2.32	12.56	1.66	5.59	78.3	8945.7	1.87	9.52
Pyraformer	24	1.75	6.92	1.83	7.88	1.30	3.58	61.8	6930.2	1.90	9.72
	72	2.47	13.03	2.67	15.39	1.52	4.97	72.0	8222.4	3.76	33.67
	120	2.77	16.04	3.00	18.95	1.59	5.37	75.1	8610.7	4.43	43.91
	168	2.95	17.95	3.20	21.06	1.61	5.56	76.4	8773.5	4.77	49.97
Informer	24	1.88	7.51	1.94	8.30	1.30	3.62	60.7	6906.9	2.01	10.56
	72	2.75	14.84	2.86	17.24	1.53	4.86	71.5	8251.4	4.24	39.24
	120	3.11	18.21	3.25	21.50	1.60	5.38	75.7	8504.5	5.15	54.31
	168	3.24	20.24	3.43	24.89	1.63	5.65	76.2	8718.4	5.26	58.42
Autoformer	24	1.93	8.64	2.06	9.57	1.42	3.97	66.5	7710.0	2.26	12.78
	72	2.72	15.14	2.97	18.38	1.54	5.14	75.4	9111.5	4.25	42.34
	120	3.21	20.27	3.34	23.12	1.58	5.73	79.2	9143.5	4.83	48.88
	168	3.43	21.71	3.56	22.55	1.64	5.95	79.8	9435.8	5.32	61.85
FEDformer	24	1.98	8.45	2.02	9.25	1.36	3.91	66.0	7384.1	2.13	11.43
	72	2.87	16.50	3.01	18.70	1.59	5.31	76.2	8824.8	4.15	37.60
	120	3.19	20.29	3.36	23.10	1.66	5.71	79.0	9143.3	4.81	48.86
	168	3.35	22.12	3.54	25.21	1.68	5.88	79.7	9189.2	5.01	53.39
PatchTST	24	2.05	9.26	2.16	10.58	1.40	4.20	66.2	7765.8	2.19	12.54
	72	2.82	16.60	3.06	19.96	1.60	5.39	75.2	9067.8	4.28	42.46
	120	3.15	20.32	3.43	24.39	1.66	5.79	77.8	9452.6	5.09	57.29
	168	3.33	22.54	3.63	26.94	1.69	6.00	79.0	9638.1	5.51	65.30
Corrformer	24	1.99	8.21	2.09	9.47	1.38	3.83	66.7	7832.3	2.19	12.39
	72	2.74	15.16	2.99	18.40	1.56	4.91	75.6	9111.7	4.27	42.36
	120	3.06	18.63	3.34	22.48	1.61	5.56	78.0	9477.4	5.08	57.13
	168	3.09	18.69	3.36	22.53	1.63	5.69	78.9	9636.0	5.34	61.83
iTransformer	24	1.82	7.49	1.93	8.80	1.32	3.77	63.2	7358.8	1.99	10.84
	72	2.60	14.46	2.84	17.50	1.52	4.96	73.2	8713.3	4.14	40.65
	120	2.97	18.36	3.24	22.16	1.59	5.42	76.4	9192.2	4.95	54.67
	168	3.18	20.64	3.48	24.89	1.64	5.67	78.0	9441.1	5.36	62.31
STID	24	4.65	40.31	4.17	34.36	1.69	6.27	79.2	9573.3	5.69	62.96
	72	4.70	41.18	4.20	34.97	1.69	6.28	79.4	9578.2	5.77	64.47
	120	4.74	41.73	4.24	35.24	1.69	6.30	79.5	9556.8	5.80	65.22
	168	4.77	42.39	4.26	35.67	1.69	6.30	79.5	9556.4	5.83	65.89
Dlinear	24	2.71	13.82	2.47	12.36	1.44	4.34	66.6	8234.5	3.09	21.34
	72	3.55	23.05	3.48	22.85	1.62	5.37	75.0	9250.8	4.64	45.83
	120	3.90	27.60	3.89	27.72	1.67	5.70	77.3	9510.6	5.19	56.22
	168	4.11	30.38	4.11	30.58	1.69	5.88	78.4	9630.0	5.48	61.73
SparseTSF	24	2.63	13.16	2.32	11.96	1.49	4.67	68.4	8655.3	3.36	24.82
	72	3.22	19.93	3.13	20.88	1.66	5.82	76.5	9905.2	5.00	53.40
	120	3.48	23.42	3.47	25.16	1.72	6.24	78.9	10290.3	5.63	66.66
	168	3.64	25.63	3.66	27.71	1.75	6.47	80.1	10485.0	5.96	73.92
TimeMixer	24	2.11	9.80	2.08	10.39	1.43	4.40	67.3	8218.1	2.28	13.37
	72	2.71	15.38	2.88	18.01	1.54	5.08	74.3	8758.5	4.14	40.05
	120	2.92	17.58	3.14	20.78	1.56	5.22	75.8	8809.3	4.78	50.49
	168	3.03	18.76	3.27	22.08	1.57	5.25	76.4	8814.9	5.04	54.87
WPMixer	24	2.21	10.65	2.19	11.15	1.49	4.75	69.7	8587.9	2.56	15.65
	72	2.81	16.51	2.97	19.02	1.58	5.31	75.4	9092.2	4.26	41.90
	120	3.02	18.71	3.24	21.82	1.59	5.36	76.8	8906.8	4.85	51.86
	168	3.14	20.12	3.38	23.40	1.59	5.38	77.1	8908.4	5.12	56.33

Table 9. Full results of all the baseline models. (Part II)

Methods	Lead Time	Temperature		Dewpoint		Wind Rate		Wind Direc.		Sea Level Pressure	
		MAE	MSE	MAE	MSE	MAE	MSE	MAE	MSE	MAE	MSE
MTGNN	24	10.53	179.46	9.71	155.53	2.15	8.66	88.0	10789.2	7.20	93.48
	72	10.30	170.35	9.50	147.95	2.09	8.19	86.1	10136.9	6.95	87.35
	120	10.26	168.87	9.47	146.95	2.08	8.13	85.9	10056.5	6.92	86.62
	168	10.24	168.29	9.46	146.52	2.08	8.14	85.9	10062.6	6.92	86.59
Chronos	24	2.19	11.20	2.21	11.94	1.50	5.08	68.8	9864.8	2.34	14.86
	72	3.00	19.97	3.26	23.75	1.74	6.76	80.8	12045.2	4.58	50.14
	120	3.36	24.52	3.70	29.65	1.80	7.23	84.7	12783.9	5.54	69.72
	168	3.58	27.36	3.94	32.94	1.83	7.47	86.5	13135.8	6.01	79.62
Timer	24	2.27	11.11	2.30	11.85	1.45	4.45	67.9	8287.0	2.87	19.77
	72	2.96	18.25	3.14	20.92	1.63	5.61	75.7	9546.6	4.79	51.24
	120	3.24	21.57	3.44	24.53	1.68	5.97	77.7	9845.7	5.45	64.30
	168	3.41	23.60	3.61	26.73	1.70	6.19	78.8	10013.4	5.79	71.72
WSSM	24	-	-	-	-	-	-	-	-	-	-
	72	2.91	17.50	3.07	20.61	1.60	5.59	73.6	8660.48	4.19	40.64
	120	3.17	20.68	3.46	24.81	1.68	5.98	76.0	9358.91	4.96	54.92
	168	-	-	-	-	-	-	-	-	-	-
UniMTD	24	-	-	-	-	-	-	-	-	-	-
	72	-	-	-	-	-	-	-	-	-	-
	120	2.03	8.66	2.03	9.31	1.37	4.03	65.95	8059.31	2.59	16.63
	168	-	-	-	-	-	-	-	-	-	-
UniTraj	24	-	-	-	-	-	-	-	-	-	-
	72	-	-	-	-	-	-	-	-	-	-
	120	2.22	8.08	2.12	8.11	1.71	4.93	84.41	10943.16	1.57	4.66
	168	-	-	-	-	-	-	-	-	-	-
PhysicsFormer (Ours)	24	1.55	5.36	1.59	6.02	1.21	3.20	57.37	6354.78	1.43	5.24
	72	2.22	10.40	2.38	12.31	1.46	4.62	69.28	7990.50	3.42	27.88
	120	2.68	14.50	2.90	17.36	1.54	5.08	73.98	8594.37	4.40	43.76
	168	2.93	17.16	3.16	20.38	1.59	5.32	76.19	8860.52	4.92	52.77



Figure 9. Visualization results of Pyraformer. Samples are randomly chosen. Orange lines are predictions and Blue lines are ground truths.

FEDformer



Figure 10. Visualization results of FEDformer. Samples are randomly chosen. Orange lines are predictions and Blue lines are ground truths.

Dlinear

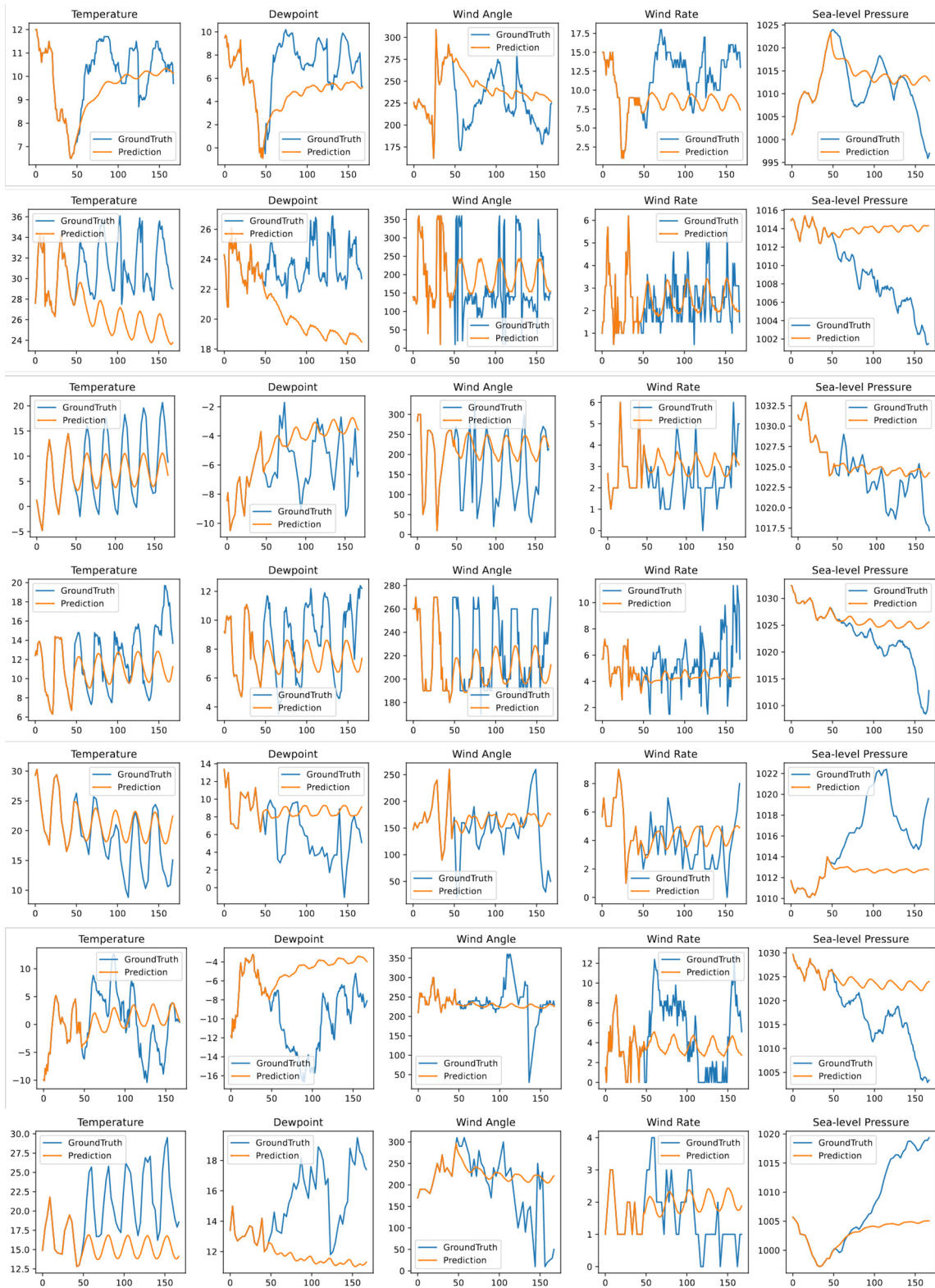


Figure 11. Visualization results of Dlinear. Samples are randomly chosen. Orange lines are predictions and Blue lines are ground truths.

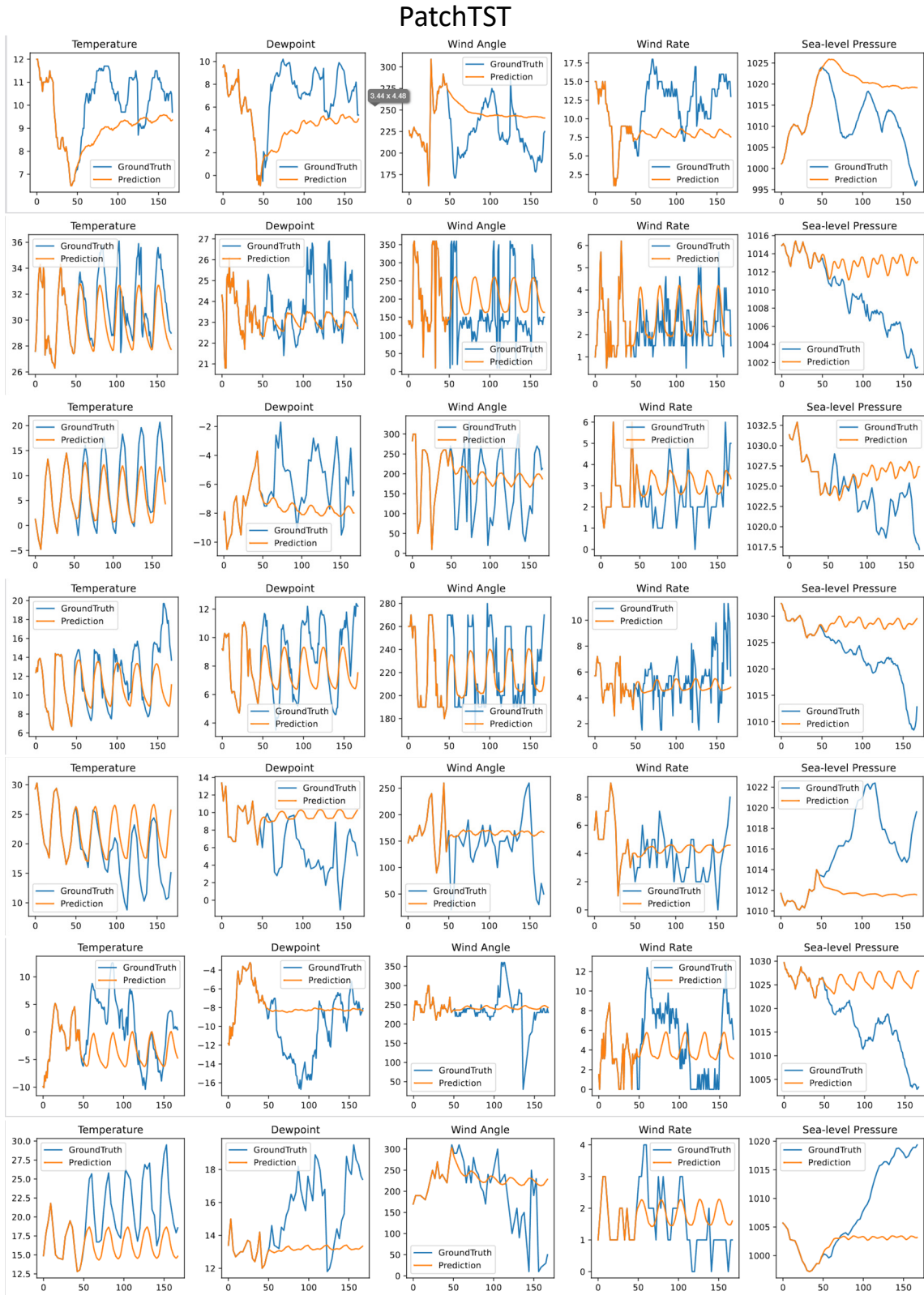


Figure 12. Visualization results of PatchTST. Samples are randomly chosen. Orange lines are predictions and Blue lines are ground truths.

iTransformer



Figure 13. Visualization results of iTransformer. Samples are randomly chosen. Orange lines are predictions and Blue lines are ground truths.

Corrformer

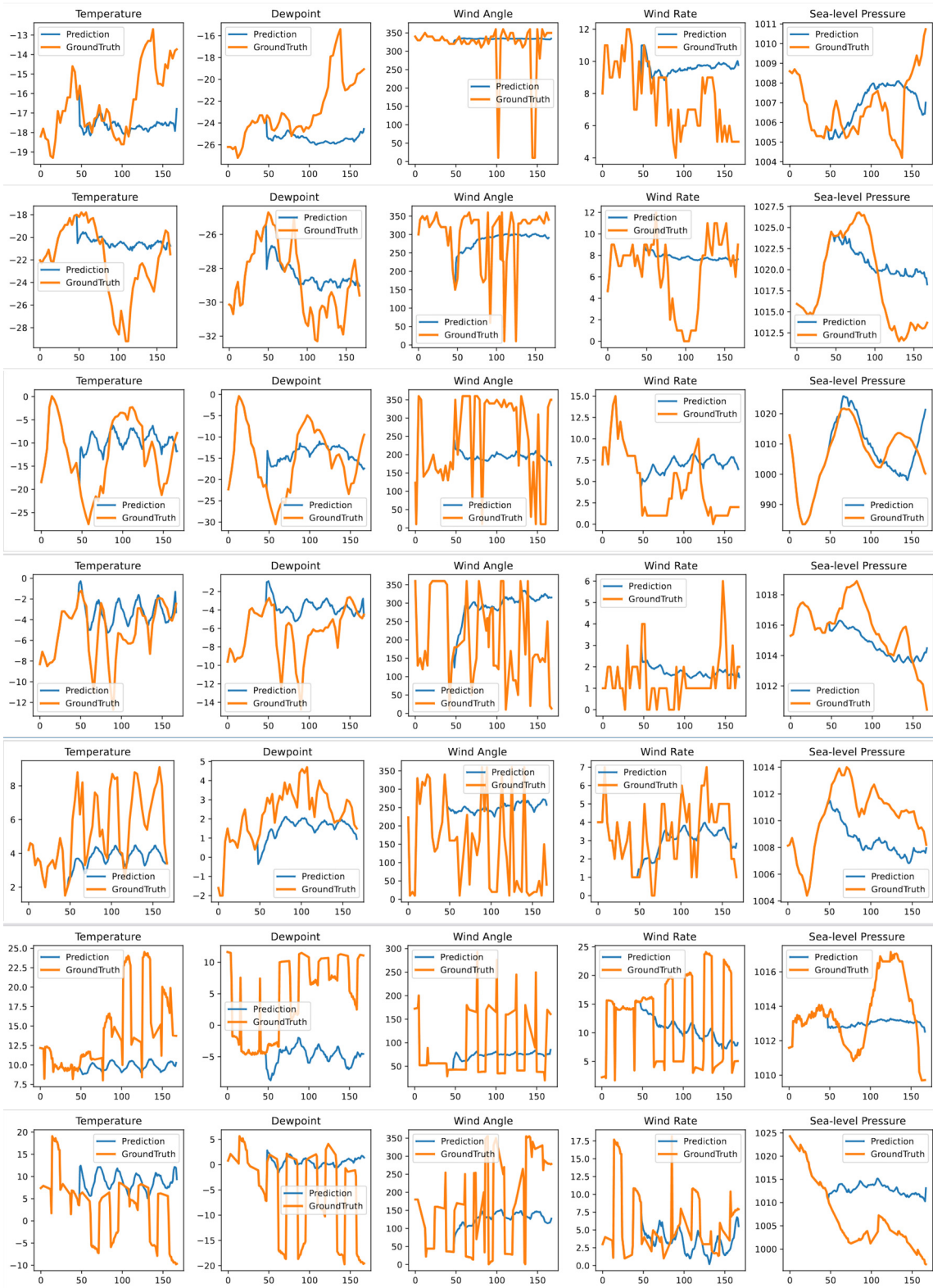


Figure 14. Visualization results of Corrformer. Samples are randomly chosen. Orange lines are predictions and Blue lines are ground truths.

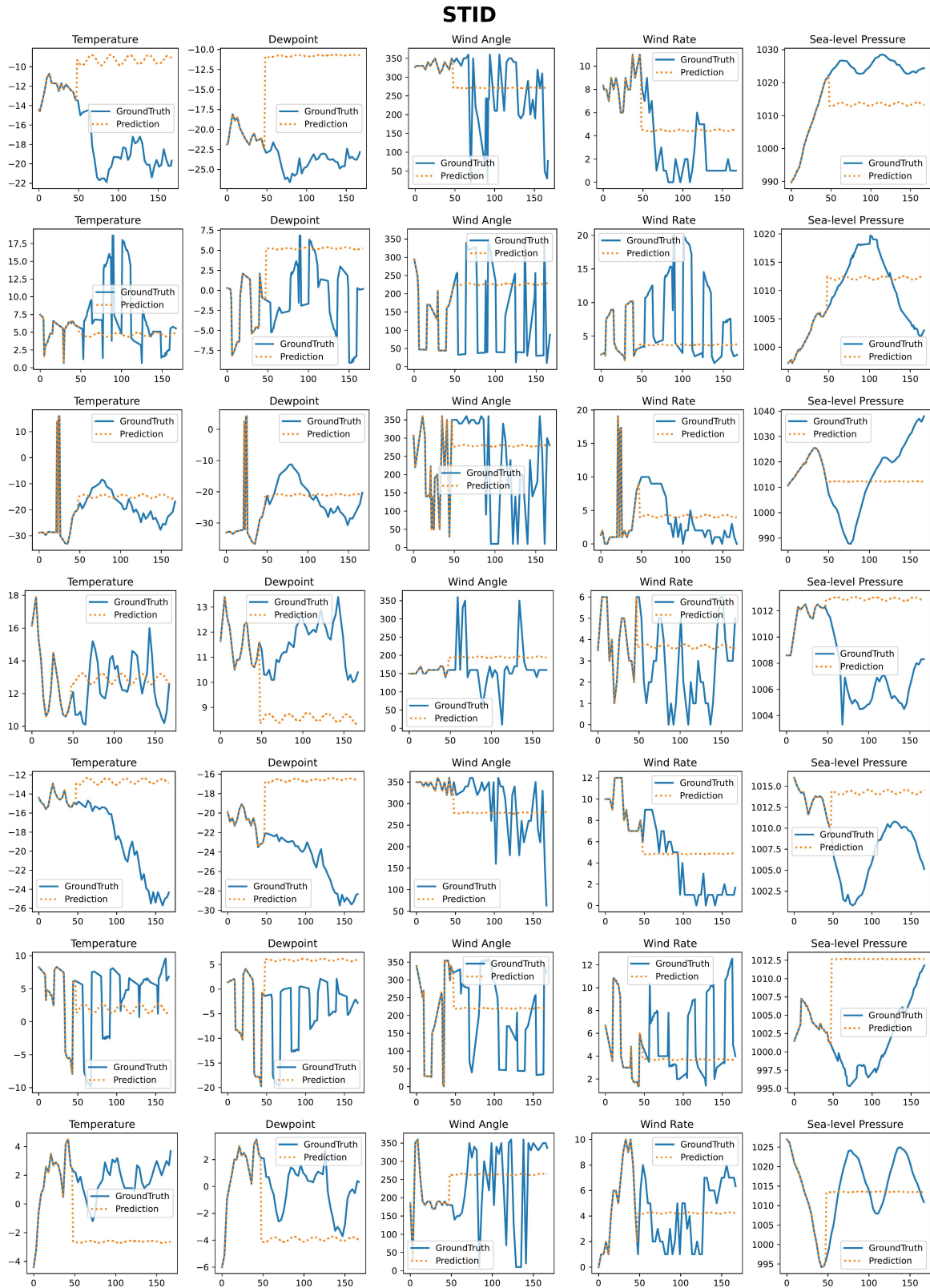


Figure 15. Visualization results of STID. Samples are randomly chosen. Orange lines are predictions and Blue lines are ground truths.

SparseTSF

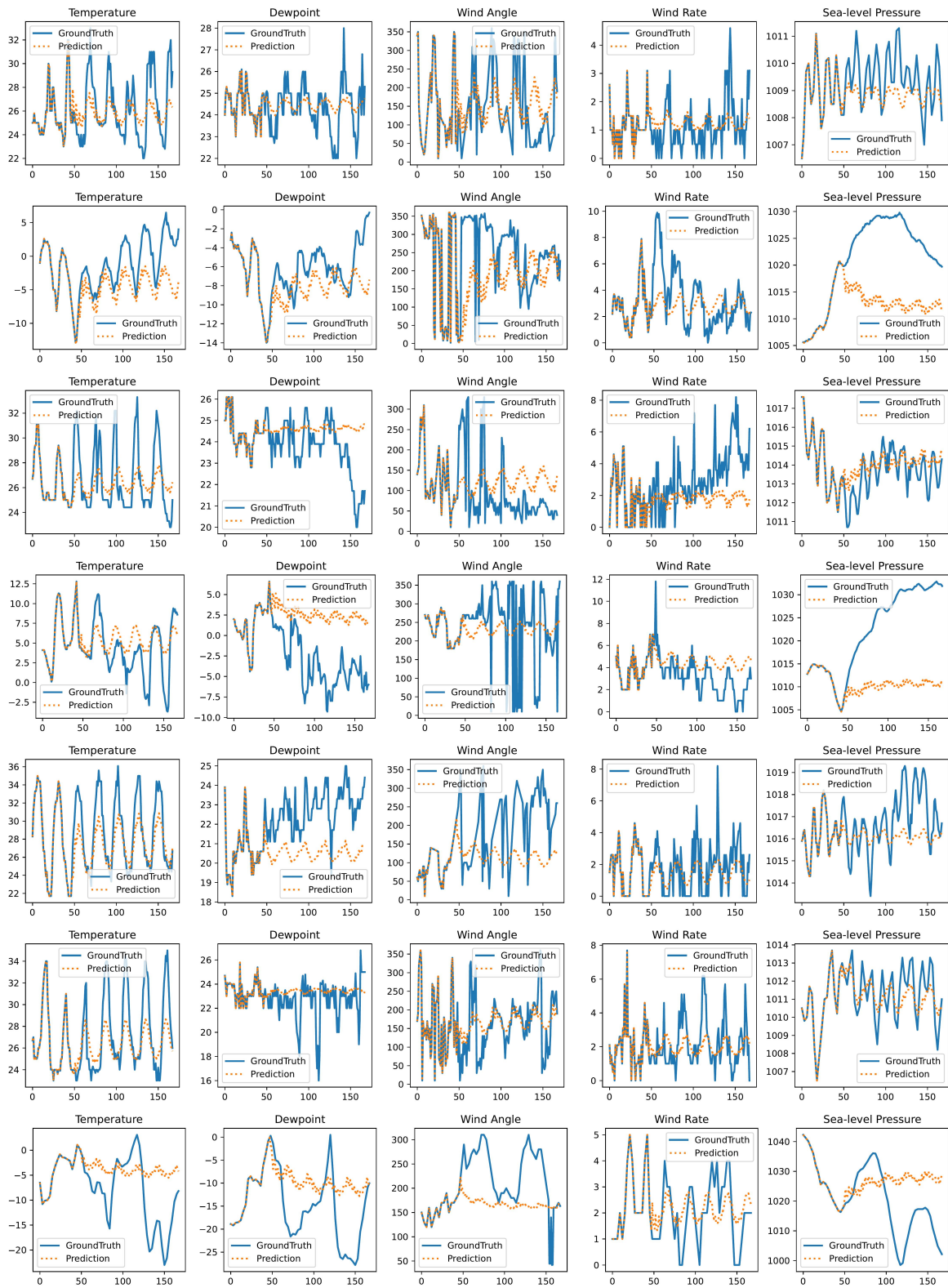


Figure 16. Visualization results of SparseTSF. Samples are randomly chosen. Orange lines are predictions and Blue lines are ground truths.

TimeMixer

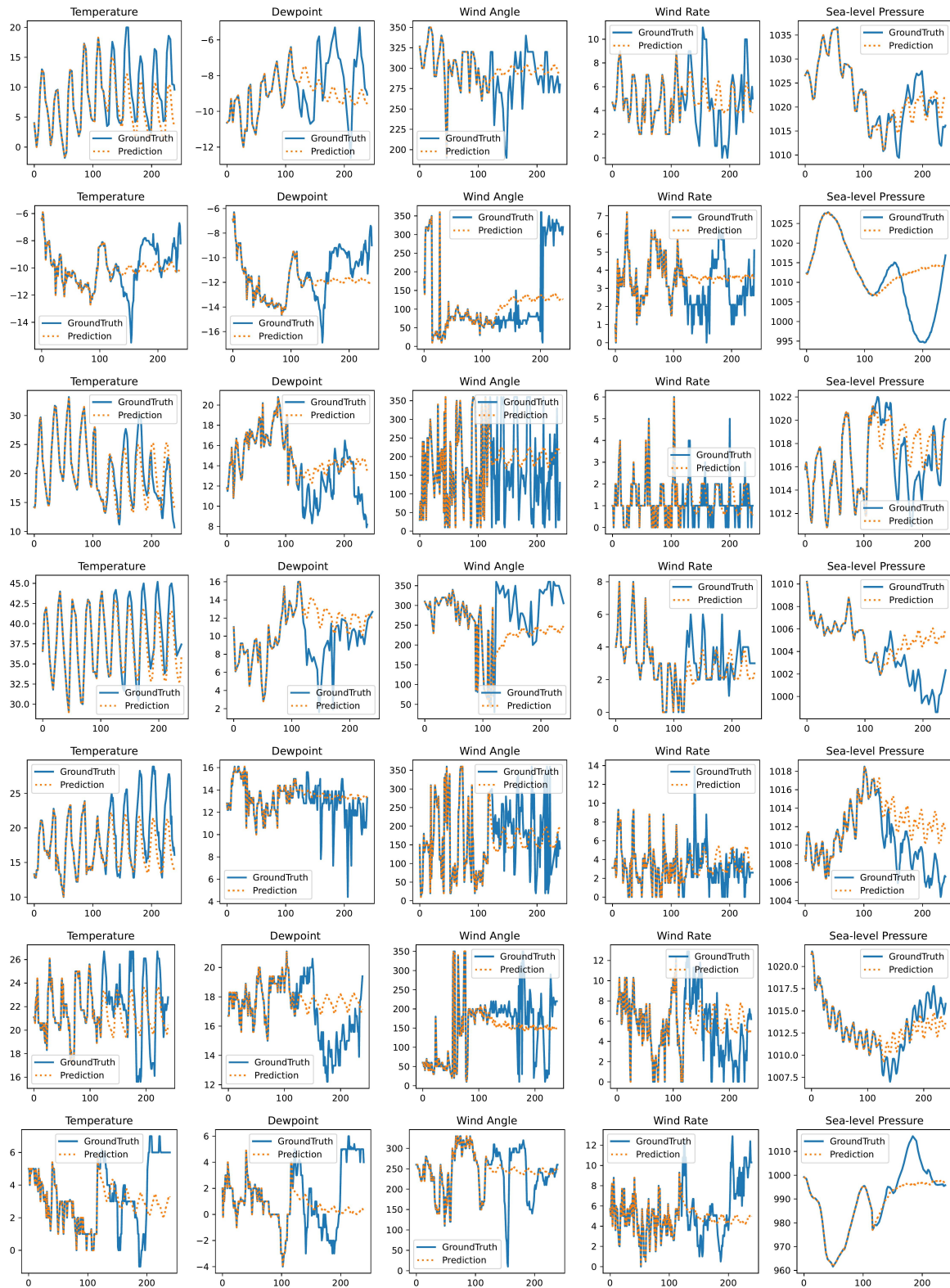


Figure 17. Visualization results of TimeMixer. Samples are randomly chosen. Orange lines are predictions and Blue lines are ground truths.

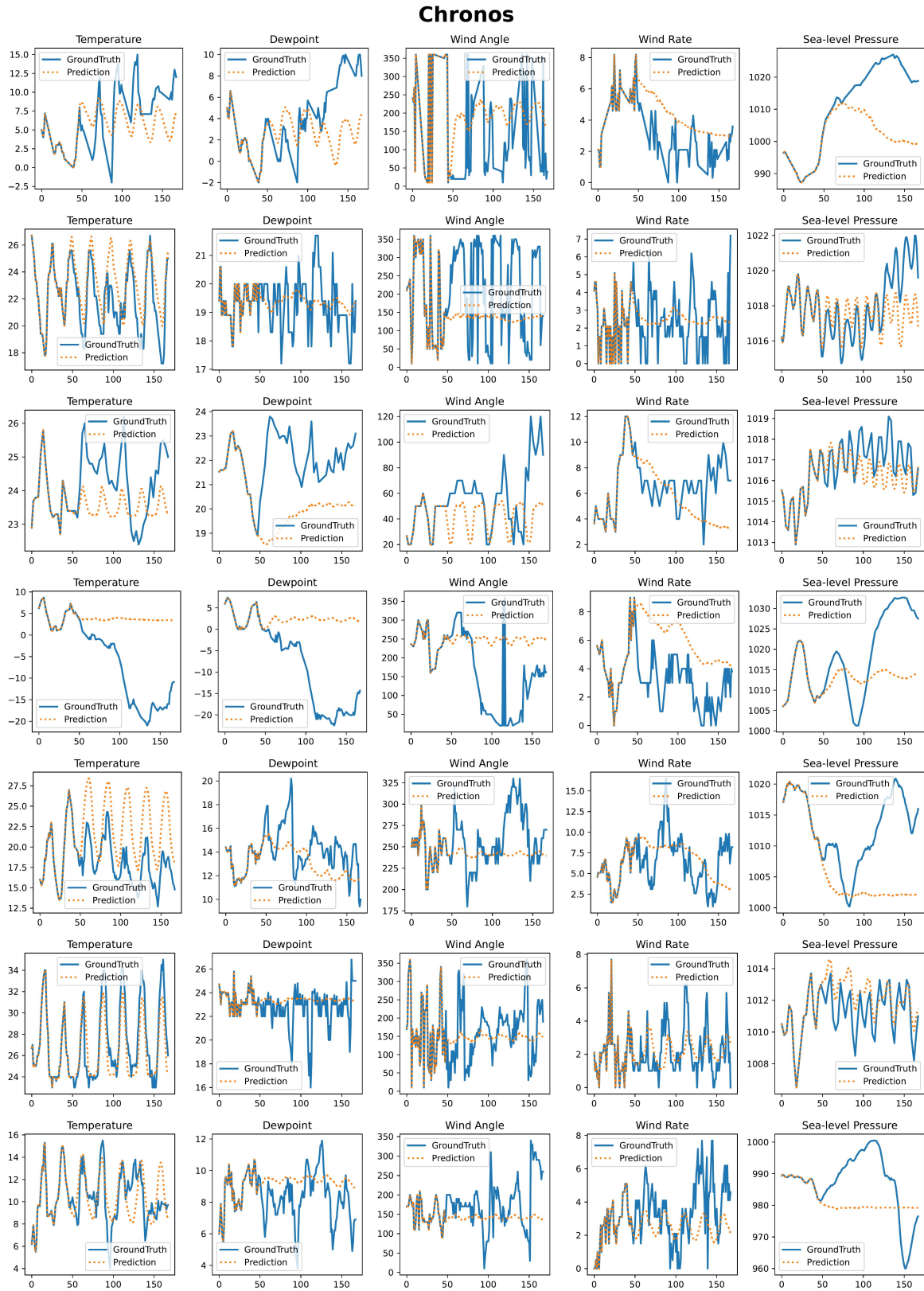


Figure 18. Visualization results of Chronos. Samples are randomly chosen. Orange lines are predictions and Blue lines are ground truths.

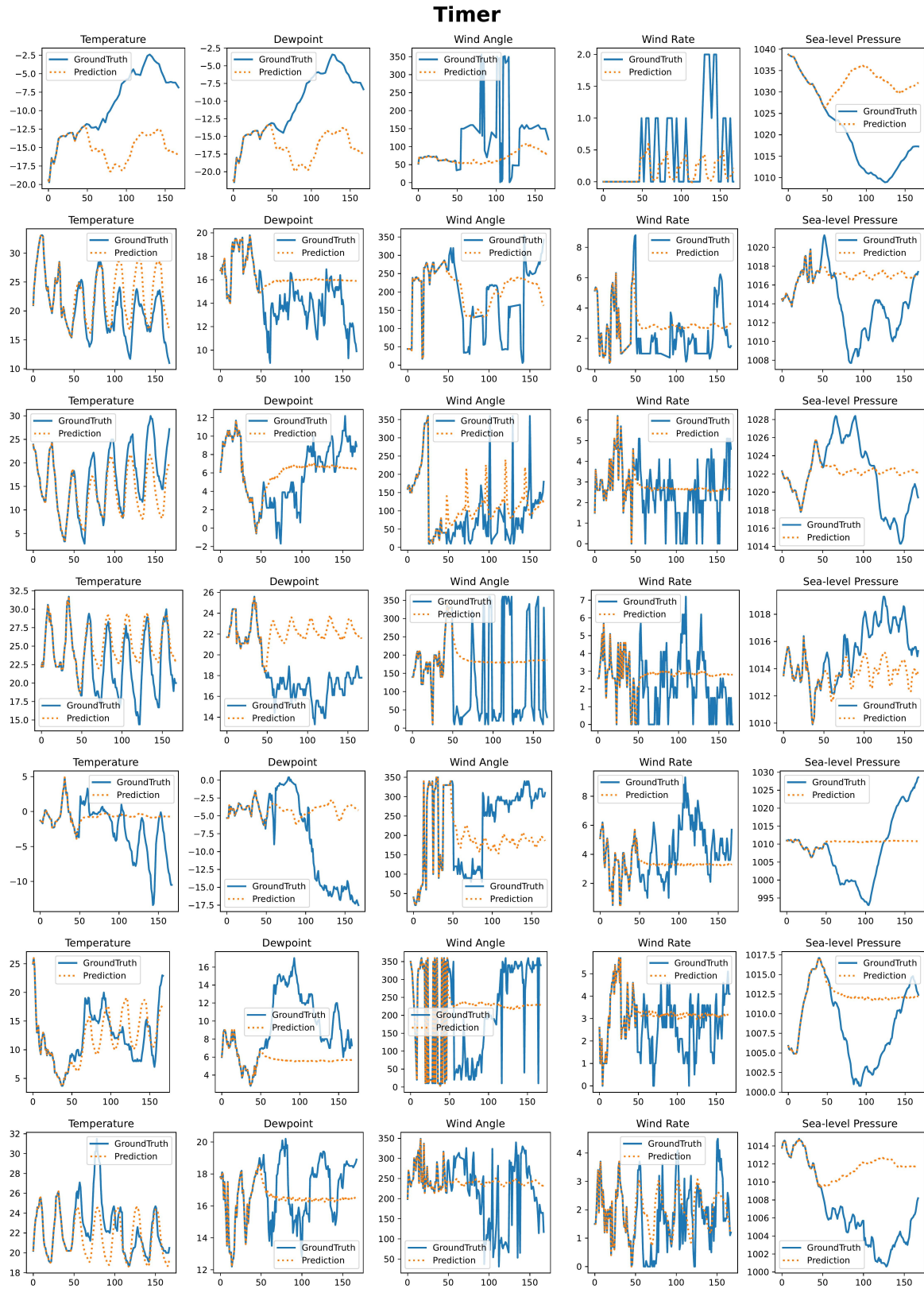


Figure 19. Visualization results of Timer. Samples are randomly chosen. Orange lines are predictions and Blue lines are ground truths.

PhysicsFormer (Ours)

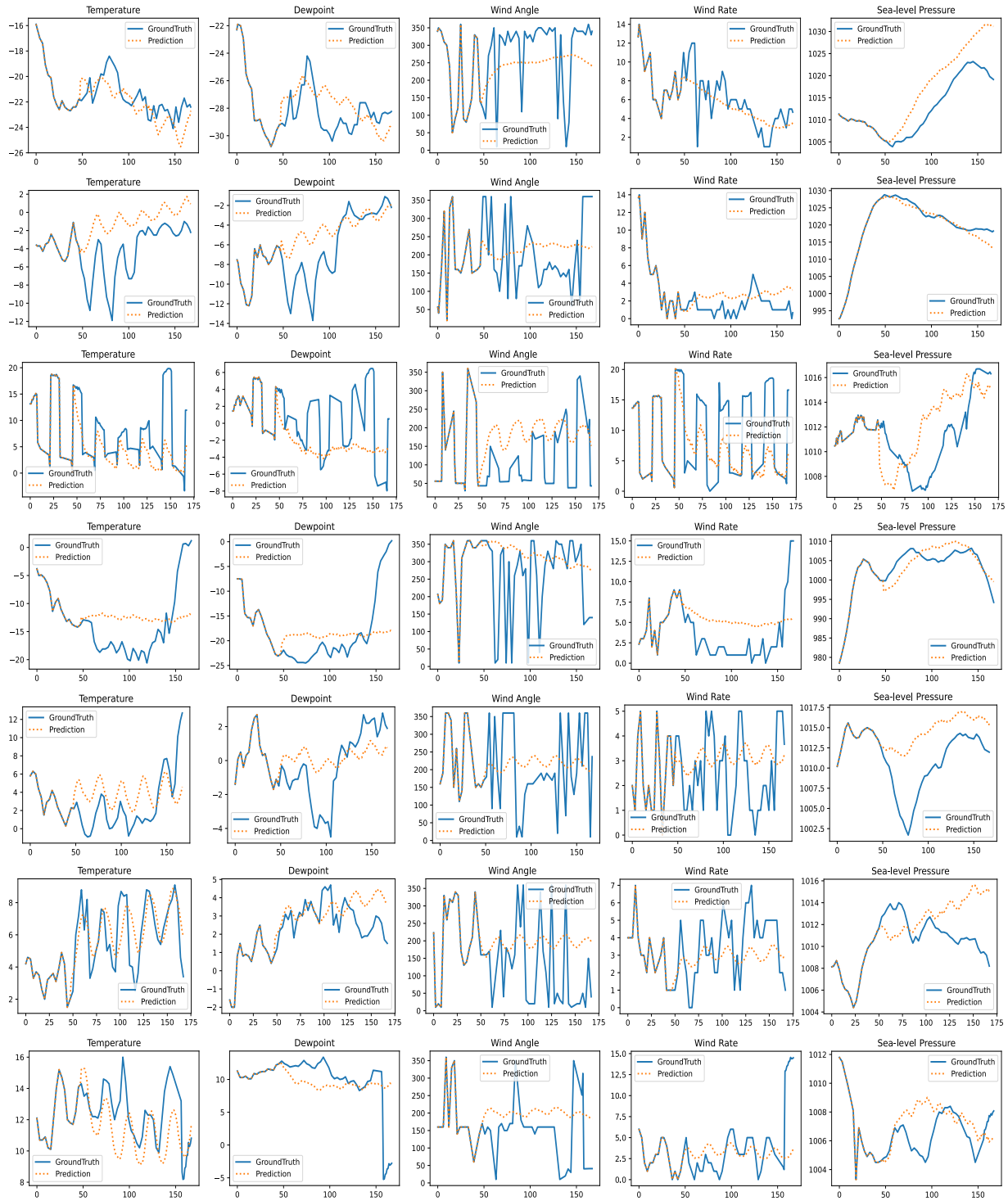


Figure 20. Visualization results of PhysicsFormer. Samples are randomly chosen. Orange lines are predictions and Blue lines are ground truths.